NASA CR-159789

SCREEN PRINTING TECHNOLOGY APPLIED TO SILICON SOLAR CELL FABRICATION

(NASA-CR-159789) SCREEN PRINTING TECHNOLOGY APPLIED TO SILICON SOLAR CELL FABRICATION Final Report, Nov. 1977 - Feb. 1979 (Spectrolab, Inc.) 64 p HC A04/MF A01 CSCL 10A G3/44

N80-27808

Unclas 28113

BY J. W. THORNHILL AND W. E. SIPPERLY

SPECTROLAB, INC.

PREPARED FOR

NATIONAL AERONAUTICS AND SPACE ADMINISTRATION

NASA LEWIS RESEARCH CENTER
CONTRACT NAS3-20826

1. Report No.	2. Government Accession No.	3. Recipient's Catalog No.
NASA CR-159789		

4. Title and Subtitle	5. Report Date
Screen Printing Technology Applied to Silicon Solar Cell Fabrication	April 1980
	6. Performing Organization Code

7. Author(s)	8. Performing Organization Report No.
Jay W. Thornhill and William E. Sipperly	
	10. Work Unit No.

9. Performing Organization Name and Address	11. Contract or Grant No.
Spectrolab, Inc. 12500 Gladstone Avenue Sylmar, California 91342	NAS3-20826

12. Sponsoring Agency Name and Address	13. Type of Report and Period Covered
National Aeronautics and Space Administration Washington, DC 20546	Final Report Nov. 1977 to Feb. 1979
	14. Sponsoring Agency Code

15. Supplementary Notes

Project Manager: John C. Evans, Jr., NASA-Lewis Research Center, Cleveland, Ohio 44135

16. Abstract

The work done on this contract optimized the process for producing space qualified solar cells in both the conventional and wraparound configuration using screen printing techniques. Process modifications were chosen that could be easily automated or mechanized. Work was accomplished to optimize the tradeoffs associated with gridline spacing, gridline definition and junction depth. An extensive search for possible front contact metallization was completed.

The back surface field structures along with the screen printed back contacts were optimized to produce open circuit voltages of at least an average of 600 millivolts. After all modifications on the process sequence that were intended were accomplished, the cells were exhaustively tested. Electrical tests at AM0 and 28°C were made before and after boiling water immersion, thermal shock and storage under conditions of high temperature and high humidity. After the tests were completed, cells from both conventional lots and wraparound lots were sent to NASA-Lewis Research Center.

17. Key Words (Suggested by Author(s))	18. Distribution Statement
Silicon, solar cells, screen printed contacts	Unclassified-Unlimited

19. Security Classif. (of this report)	20. Security Classif. (of this page)	21. No. of Pages	22. Price*
Unclassified		58	

* For sale by the National Technical Information Service, Springfield, Virginia 22151

TABLE OF CONTENTS

LIST OF FIGURES

LIST OF TABLES

ABSTRACT

The work done on this contract optimized the process for producing space qualified solar cells in both the conventional and wrap-around configuration using screen printing techniques. Process modifications were chosen that could be easily automated or mechanized. Work was accomplished to optimize the tradeoffs associated with gridline spacing, gridline definition and junction depth. An extensive search for possible front contact metallization was completed.

The back surface field structures along with the screen printed back contacts were optimized to produce open circuit voltages of at least an average of 600 millivolts. After all modifications on the process sequence that were intended were accomplished the cells were exhaustively tested. Electrical tests at AMO and 28^{o}C were made before and after boiling water immersion, thermal shock and storage under conditions of high temperature and high humidity. After the tests were completed, cells from both conventional lots and wraparound lots were sent to NASA-Lewis Research Center.

1.0 SUMMARY

An optimized screen printing process was developed for use on space solar cells. This process was effective with both the conventional solar cell and the wraparound cell. All experiments that did not specify the number of cells used were run with five cells for each data point. All cells used were AR coated.

The cells fabricated under this contract performed well under the conventional Scotch tape peel test, storage at 80°C and 90% relative humidity for ten days, a ten minute immersion in boiling water and thermal shock consisting of fifteen cycles from -196°C to +100°C at a 20°C/minute rate.

The cells fabricated for both the lot of conventional cells and the lot of wraparound cells used a texturized surface. This step reduced the reflectivity at the surface and improved adhesion of the front surface metallization. This program also found that it was necessary to tighten the specification for the bulk resistivity of the wafer. Nine to fourteen was suggested instead of the seven to fourteen which was used in the past. The higher resistivity bulk material was somewhat less sensitive to the mechanical processes associated with screen printing.

Work was also completed on the trade-offs that must be considered between cell output, junction depth and minimum gridline width. Eight to ten lines per centimeter proved to be the minimum density of gridlines that would permit the use of a shallow junction. A screen mesh size of 325 and a mesh orientation of 22° was used to give the proper line definition. The emulsions used had a thickness of 0.020 to 0.025mm. The paste was dried with a fast infrared drying cycle which caused the exterior of the paste to harden first, preventing paste flow during drying.

A number of different pastes were looked at as possible candidates for the front surface metallization. These pastes included selections from various non-silver materials, commercially available silver compositions, modified silver compositions, modified frit compositions, diluted and modified frit compositions and customized frit compositions. Thick Film Systems paste A256 with Transene n-diffusol was selected from the modified frit composition group as the paste that had the best overall characteristics. Frit content not exceeding five percent and firing temperature not exceeding 700°C were determined as the optimum characteristics for this paste.

Work completed on the optimization of the back surface field processing sequence has shown that the back etch step before printing of the aluminum is optional. No noticable degradation of the curve shape can be seen when the step is left out of the process. Open circuit voltages of greater than 600 mV have been obtained with both variations.

A minimal amount of work was also done to determine the minimum cell thickness with acceptable yields. Cells 2½ to 3½ mils were the thinnest that could be reproduced with any consistency. Work on the dielectric isolation used for the wraparound configuration proved Thick Film Systems 1126RCB superior to the others tested. A double coating was preferred for filling in pinholes and eliminating shunting effects.

The process sequence optimized under this contract was used to fabricate a lot of both conventional and wraparound cells. Thirty cells electrically tested, ten cells tested in boiling water, twelve cells tested in high temperatures and high humidity and five cells exposed to a thermal shock cycle were selected from the initial lot of conventional cells and shipped to the NASA-Lewis Research Center.

Twenty-five cells were selected from the lot of cells with the wraparound configuration and tested for electrical performance at AMO and 28°C. These cells were also shipped to the NASA Lewis Research Center. Other cells from the lot of wraparound cells were tested in boiling water and exposed to thermal shock tests, but no testing at high temperature and high humidity was accomplished due to a lack of additional funds and time.

2.0 INTRODUCTION

2.1 BACKGROUND

Future space missions are currently being planned that will require the use of very large quantities of solar cells. Programs such as the Solar Electric Propulsion System (SEPS)[1] and the Satellite Solar Power System (SSPS)[2] will require the manufacture of such large numbers of cells that it becomes highly desirable to develop cell designs and processing techniques that are amenable to automated or mechanized fabrication. Current aerospace solar cell processing involves considerable hand labor and individual device handling, particularly in the high vacuum deposition of contact metallizations and antireflective coatings.

Screen printed contact metallizations are in common usage for the manufacture of terrestrial silicon solar cells. This technique is one that has been shown to be amenable to automation by investigations at Spectrolab, discussed in the NASA-Lewis final report, "Demonstration of the Feasibility of Automated Silicon Solar Cell Fabrication", under contract NAS3-18566.[3] Contract NAS3-20029, also sponsored by NASA-Lewis, demonstrated that screen printed silicon solar cells could be fabricated with significantly improved characteristics, as well as with a screen printed dielectric wraparound configuration that permitted wraparound contacts.[4] This wraparound contact structure offers the possibility of major savings in solar panel assembly using automated procedures.

While the feasibility of these concepts was shown by these efforts, the processes and materials used were not optimized. It was necessary to use relatively deep junctions to avoid shunting effects brought about by firing on the screen printed contacts, with the associated penalty of reduced conversion efficiencies. Also, no real attempts were made to reduce gridline widths in order to increase cell active areas. Some environmental tests were performed, but the effects of boiling water immersion, thermal shock, and storage under conditions of high temperature and humidity were

established only for the specific pastes in use at that time. No work was done to investigate a variety of screen printed pastes for contacts and for dielectric isolation.

2.2. OBJECTIVES

This investigation was carried out with the specific intent of developing screen printed metal front and back contacts that met the following requirements:

- grid line widths were to be minimized to the limit of the state-of-the-art for screen printing technology
- contact coverage of the front surface area was to be less than 10%
- cell series resistance was to be equal to or less than that of conventional vacuum metallized cells
- the screen printed metallization was to have a sheet resistance less than 0.02 ohm/square, and the metal-to-silicon contact resistance was to be less than 0.02 ohm-cm^2
- back surface field structures along with the screen printed back contacts should produce open circuit voltages of at least 600 millivolts (average) for 10 ohm-cm silicon base material
- the contact paste material should not cost more than $0.05 for 60 cm^2 of cell
- contacts were to withstand the standard Scotch tape peel test
- contacts were not to be adversely affected by humidity
- the screen printed contacts were to exhibit low resistance ohmic behavior

The silicon solar cells to be used for the investigation were to be 2 X 2 X 0.02 cm in size, with the n^+ diffused layer having a sheet resistance of approximately 100 ohms/square, both being typical for current space cell production. Texturization of the front surface was optional. Paste composition, printing screens, printing conditions, firing procedures, and firing atmospheres

were to be optimized for solar cell applications. If possible a single contact firing was to be utilized.

The minimum thickness of silicon to which such screen printed contacts could be used was to be established. The screen printed contacts were to be capable of withstanding the conventional Scotch tape peel test, storage at 80°C and 90% relative humidity for ten days, a ten minute immersion in boiling water, and thermal shock consisting of fifteen cycles from -196°C to +100°C at a 20°C/minute rate without loss of adhesion.

A thick film dielectric paste was to be developed and used to provide isolation for screen printed wraparound contacts. This dielectric material was to be pinhole-free and provide more than 10^5 ohms isolation with a thickness of less than 30 microns. In the wraparound configuration the dielectric should not show beading along the edge of the cell after firing, and should be compatible with the metallization. No loss in isolation should occur after the temperature/humidity storage test.

Once the materials and processing had been optimized, two groups of cells were to be fabricated utilizing these materials and processes. One group was to be in the conventional non-wraparound configuration, and the other was to be with wraparound contacts using screen printed dielectric isolation.

2.3. PROGRAM ORGANIZATION

In order to attain the objectives of the program, the effort was divided into the following specific tasks:

Task I Optimize the composition of the pastes, the dimensions and type of screen mesh, the printing conditions, the metal type and composition, the curing conditions, the firing schedule and atmosphere to obtain the desired

contact characteristics and apply the optimized process to fabricate silicon solar cells. Establish the minimum thickness of silicon to which such contacts can be applied without breakage. Perform an evaluation of the cells and contact system, testing for electrical performance, effects of boiling water immersion, storage under elevated temperature and relative humidity, adhesion and thermal shock.

Task II Develop an appropriate dielectric paste and the process for applying it and firing it to permit the fabrication of dielectrically isolated wraparound contact cells, to be made using only screen printing techniques.

Task III Using the processes, materials, and techniques developed under Tasks I and II fabricate 24 silicon solar cells in the non-wraparound configuration, and 25 cells with wraparound contacts.

3.0 TECHNICAL DISCUSSION

3.1 JUNCTION DEPTH OPTIMIZATION

It was decided early in the program that the front surfaces of the cells used in this program should be texturized. This improves the short circuit current because of reduced front surface reflectivity. It also permits screen printed contacts to "key" to the surface and thus should improve adhesion. The starting material was therefore first etched with a 30% sodium hydroxide solution at about 110°C to remove saw damage. A 2% sodium hydroxide solution containing 20% isopropyl alcohol was then used to develop the texturized front surface of the cells. The alcohol is added to precipitate the sodium silicate reaction product. This low concentration NaOH etchant is orientation dependent and develops a surface that is uniformly covered with closely packed tetrahedra when used on a silicon surface that is in the (100) plane.

As might be expected, texturized surfaces are more sensitive to handling than smooth surfaces because of the possibility of damage to the peaks of the tetrahedra. Past experience has also shown that this sensitivity to mechanical damage is greater for silicon having lower bulk resistivity. The sensitivity also increases with shallow diffusions. It was desirable, therefore, to explore both the effects of junction depth and bulk resistivity for screen printed contact cells.

An experiment was performed which compared 1-3 ohm-cm with 9-11 ohm-cm materials. A series of diffusions were made with the two materials, yielding sheet resistance values of 40, 60, and 80 ohms/sq. Cells were then fabricated using screen printed contacts of Engelhard #A-2921 paste and aluminum paste P^+ back surface field structures with the fired-on aluminum left in place to act as the back contact. The results of these tests are given in Table 1 below:

Table 1

Effect of Bulk Resistivity and Junction Depth

Junction Depth	Bulk Resistivity	Average CFF	Scatter in Max. Power Current
80 ohms/square	2 ohm-cm	.68	11 mA
	10 ohm-cm	.71	5 mA
60 ohms/square	2 ohm-cm	.70	5 mA
	10 ohm-cm	.72	3 mA
40 ohms/square	2 ohm-cm	.72	3 mA
	10 ohm-cm	.74	2 mA

Since the paste used was not optimized, the cells had relatively poor curve fill factors, however, the data show a clear trend that the higher resistivity material is somewhat less sensitive to the mechanical processes associated with screen printing. Normally silicon having a bulk resistivity of 7 to 14 ohm-cm is classified as ten ohm-cm material. The results of these experiments indicated that it would be prudent to tighten this specification to 9 to 14 ohm-cm in order to improve yields and permit the use of shallower junctions.

A trade-off must be performed in normal solar cell design between cell output and junction depth for a given minimum gridline width. With screen printed contacts, an added constraint appears, because of shunting effects with very shallow junctions. Present printing techniques are not capable of producing lines much narrower than 0.13 mm after firing. Increasing the gridline density will permit the use of shallower junctions (improving cell output) without seriously increasing series resistance. But if gridlines cannot be made narrower, losses in active area start to become objectionable.

In order to investigate this effect for a gridline width of 0.13 mm, a series of diffusions were made using 10 ohm-cm, texturized wafers.

The wafers were 0.20 mm thick and aluminum paste back surface fields were used. The wafers were then fabricated into 2 X 2 cm cells using a series of different gridline densities. Using 0.20 ohm as a reasonable upper limit for cell series resistance, the minimum number of grid lines was established for the various junction depths. These data are shown below in Table 2.

Table 2

Minimum Number of 0.13 mm Gridlines for Various Junction Depths

Junction Depth (ohms/square)	Minimum Number of Lines per 2 X 2 cm Cell
30	5
40	6
55	10
70	12
100	16

Measurements of the short circuit current for the test cells at AMO also gave an indication of the effect of junction depth on cell output for illumination containing an appreciable ultraviolet content.

Table 3

Short Circuit Current vs Junction Depth

Junction Depth (ohms/square)	Short Circuit Current (mA/cm^2)
30	38.1
40	39.0
55	40.2
100	41.6

The combined data appear to indicate that a junction depth of about 45 ohms/sq., along with a minimum of three gridlines per centimeter, should provide the best compromise for a line width of about 0.13 mm, providing a satisfactory photocurrent and an acceptable series resistance. In order to permit additional shallowing of the junction, it was decided to use a gridline density of eight to ten lines per centimeter.

3.2 Gridline Definition Considerations

Several factors must be considered basic in the choice of a printing screen. These are mesh size, the thickness of the emulsion, the orientation of the screen mesh with respect to the pattern, the paste rheology, and the drying procedures used. It was found that a mesh size of 325 gave satisfactory prints for most of the pastes investigated. Coarser mesh screens, such as 200, were found to give some loss in line definition due to the thickness of the deposit and the resulting tendency for spreading. Finer meshes (i.e., 400-mesh) were found, in some cases, to have a pore size not sufficiently wide to pass some of the larger particles in some pastes, and thus gave some problems with "plugging". This caused voids or pinholes in the prints if not cleared immediately by cleaning. By using a lower viscosity paste, some pinholing could be avoided, but this also brought about line spreading and losses in definition. Commercial paste manufacturers recommended a line pattern width of 0.10 to 0.13 mm, a mesh size of 325, and a mesh orientation other than 90^{o} to the line pattern for maximum definition. The final screens used had an orientation of 22^{o} to the line patterns to avoid having a screen wire or a series of wire crossovers exactly coinciding with pattern openings. The emulsions used had a thickness of 0.020 to 0.025 mm. Such screens were found to give acceptable line resolution and uniform line widths.

Procedures used for paste drying prior to firing were found to have a marked effect on the line definition that could be attained. Oven drying, while used on this program since it was the easiest and readily available, does allow some lateral flow of the paste before the solvent vehicle is completely driven off. A better procedure would have been to use a fast infra-red drying cycle, which causes the exterior of the paste to harden first, preventing paste flow during drying.

The viscosity of the paste was also found to have a marked effect on line definition, with the lower viscosity inks having some tendency to flow or "spread" after printing. Too high a viscosity results in insufficient flow after printing to give the needed leveling to eliminate screen marks and variations in paste depth. A common practice among paste manufacturers is to include a thixotropic component in the paste. This produces a lowered viscosity under the shear forces of the squeegee, yet causes the paste to set up again after these forces have passed. Such pastes remain well mixed in their containers because of the high viscosity, but still flow very well under the action of the squeegee. It is a good practice, however, to print several patterns on dummy wafers before actual use to assure good ink flow and leveling on actual cells.

A variety of commercially available conductive pastes were compared from the following suppliers:

AVX Materials	Ferro Corp.
Cermalloy	Methode Development Co.
E.I. DuPont De Nemours	Plessey EMD
Electromaterials Corp.	Thick Film Systems
Electro-Science Laboratories	Transene Co.
Engelhard	

What appeared to be the best rheology was found for the materials from Thick Film Systems and from the Ferro Corporation's thermoplastic inks. Comparable line widths were obtained with both of these materials. Since the thermoplastic inks from Ferro required specialized printing equipment, it was decided to use only conventional inks for this investigation.

3.3 EFFECTS OF FRIT CONTENT AND FIRING CONDITIONS

A curve fill factor of .68 to .76 can be obtained if the glass frit content of the paste is not more than five percent and if

the firing temperature is not higher than 700°C. Those inks designed for use on glass substrates appear to be the most useful for solar cell applications.

In general, for a given firing temperature, the short circuit current will increase as the firing times are increased. As the maximum I_{sc} is approached, the series resistance starts to decrease, and a moderate value of curve fill factor will be obtained, ranging from .68 to .76. Further increases in the firing time results in decreasing values of I_{sc} with little change in the CFF until finally shunting begins to appear, with losses in fill factor. The initial decrease in the short circuit current may, from other investigations, be associated with the partial shunting of the junction and localized higher junction fields. For most pastes, the maximum in I_{sc} does not occur simultaneously with the maximum in CFF. It was found that for pastes that were highly sensitive to firing times, the maximum fill factor was achieved after the short circuit current had started to fall off. It was quite possible therefore, for a paste that did not give the best line definition to give a better performance in terms of the finished cell characteristics.

The fall-off in short circuit current appears to correlate well with the paste frit content. Paste materials appear to bond to the silicon surface by an oxidative reaction. The frit composition determines the rate and magnitude of the silicon oxidation. Other factors which may be present are lattice distortion or impurity migration, the latter possibly causing the changes observed in short circuit current which occur without changes in fill factor. Most of the frit materials found in pastes contain lead oxide which can be reduced by silicon to yield silicon dioxide and elemental lead. In the presence of oxygen the lead is oxidized again to continue the reaction with silicon. Some verification of this effect has been done by firing the paste materials for a constant time in atmospheres containing varying levels of oxygen. Increased shunting was found for increased oxygen levels, with the

scatter in maximum power levels increasing also for increased oxygen content. As the firing atmosphere was made to contain higher and higher percentages of nitrogen, it became necessary to increase the firing temperature in order to avoid curve fill factor degradation from increased series resistance. Increased firing times for the same firing temperature were not capable of compensating for increased nitrogen content in the firing atmosphere.

The optimum firing time appears to be a moderately stable factor, and the firing temperature can be varied to compensate for ambient changes. The best fill factor and tolerance to variations was tested for each paste as a function of atmosphere firing times and temperatures. No really significant advantage was found by shifting to a nitrogen rich atmosphere, and thus optimized firing schedules were established using an air ambient, primarily because of the potential versatility and cost savings. Preliminary tests of the effects of humidity appeared to indicate also that nitrogen fired metallizaticns were more subject to output degradation than air fired parts.

The organic vehicle and binder used in commercial paste materials do not appear to play a role in the output characteristics of finished cells. It thus becomes possible to combine an optimized frit material and content with a binder having an optimum rheology. Thus an improvement in cell output due to a reduced gridline width is not compromised by an improper silicon-frit interaction.

3.4 BACK SURFACE FIELD FORMATION

The back surface field obtained by alloying screen printed aluminum paste, a process developed under contract NAS3-20029, was utilized and refined to produce open circuit voltages greater than 600 mV.[4] This process was used to produce space qualified cells ranging in base resistivity from one to eight hundred ohm-cm. It was found possible to carry

out this process without the necessity for a back etching step, because the molten silicon-aluminum eutectic can penetrate as much as 15 micrometers into the back surface of the cells. The phosphorus-diffused layer is overrun and dispersed into the melt in the process.

Wafers are fired in a horizontal position using a "skeleton" boat which has minimal thermal mass, this allows the time temperature cycle to be essentially a "spike". The silicon regrowth layer is doped to saturation with aluminum, producing an abrupt P^+/P back surface junction. The epitaxial regrowth silicon layer is very thin, with the remainder of the silicon forming a dendritic silicon layer. The aluminum then forms a metallic layer as an overlay. The large thermal mismatch between the thermal expansion coefficients of aluminum and silicon are at least partially compensated for by the porous nature of the aluminum, a high aluminum oxide content, and the natural malleability of the aluminum.

A layer of aluminum oxide powder forms on the surface of the alloyed aluminum paste. This must be removed in order to obtain a low resistance contact to the cell. Treatment with dilute sodium hydroxide followed by ultrasonic agitation can be used to remove this powder, but high level ultrasonic cleaning can damage the front surface tetrahedra on texturized cells. By going to 325-mesh aluminum powder in the paste, and using a warm 1% NaOH treatment for only a short time, a gentle ultrasonic cleaning may be used. The powder was found to be readily removed also by rubbing the back surface with a mild abrasive, such as baking soda. The remaining back surface is then a bright metallic aluminum layer.

Several experiments were attempted to simultaneously fire both the screen printed aluminum and back and front metallizations, where each had been dried immediately after printing. This does not appear to be practical because of the disparity between

optimum firing times and temperatures. Some co-firing was accomplished by using a nitrogen atmosphere, but the resulting back surface exhibited almost no field effect.

3.5 PASTE COST CONSIDERATIONS

The typical quantity of aluminum paste required to achieve a high quality back surface field is approximately 0.01 gm/cm^2. This consists of 6.6 mg/cm^2 of aluminum powder and 3.4 mg/cm^2 of organic materials for the vehicle and binder. If the aluminum powder, ethyl cellulose binder, and terpineol vehicle are purchased separately and mixed in-house, the cost of coating 60 cm^2 of back surface will be about 1/3 of a cent for the materials. Aluminum paste without any glass frit content may be purchased commercially. In modest quantities the cost of using such a paste to cover 60 cm^2 would be about 8 cents, however, prices are subject to change.

Typical silver paste deposition quantities are 0.01 gm/cm^2 when using a 200-mesh screen with a 0.025 mm thick emulsion, which might be considered an upper limit on contact paste thickness. Actually a 325-mesh screen, which produces a thinner deposit, would most likely be used. If it is assumed that the front contact coverage is a full 10% of the cell area, then a typical silver metallization (i.e., Thick Film Systems A256 + 2% Transene n-diffusol), which costs about 84.7 cents per gm, would cost approximately 5.08 cents for 60 cm^2 of cells. If it is also assumed that the same silver paste would be applied to the backs of the cells, and that a 95% back surface coverage is used to provide some contact "float", then 60 cm^2 of 2 X 2 cm cells can be metallized for about 13.37 cents.

The above figures are necessarily approximations, since the amount of paste used will depend on whether the screen printing operations are continuous or start-stop, with frequent screen cleaning

required. The prices of commercial pastes are also sensitive to the quantities purchased at any one time.

3.6 NON-SILVER METALLIZATIONS

Because of the relatively high cost of silver pastes, some attempts were made to evaluate the use of base metal pastes for cell contacts. Copper and nickel conductive pastes were purchased from the Transene Company and tested. Both of these materials require a relatively high firing temperature and must be fired in an inert atmosphere. A time-temperature matrix was investigated for both pastes, but no firing schedule could be found that did not result in shunting and extremely poor I-V characteristics. It was felt that these pastes were potentially cheaper than silver paste, and thus worth testing, but the poor results obtained indicated that appreciable effort would be necessary to develop a viable process.

Aluminum-silicon alloy and molybdenum-aluminum alloy pastes were also tested for possible use as front grid contacts. Time-temperature matrices were investigated in inert atmospheres. The aluminum-silicon material gave more shunting than the aluminum molybdenum alloy, but both showed curve fill factors less than .68 and were judged unsatisfactory. It had been hoped that these materials could be used, since they offer a freedom from including glass frit in the paste. It might be possible to use the aluminum alloy pastes for contacting P-on-N structures, but this was not investigated because it was beyond the scope of the program. The lack of immediately encouraging results and the complexities of the problems made it necessary to restrict the development effort of this program for front contacts to silver conductive pastes.

3.7 GLASS FRIT MATERIALS

The nature of silver paste contacts requires frit. It is possible to use fritless silver paste, fired at temperatures as high as

the melting point of silver, and get good I-V curve shapes, but the contacts will not adhere after exposure to humidity. Adherence is dependent on some fusion of the frit with the silicon which produces some dissolution of the silicon through an oxidative sequence. The silicon dioxide formed during the firing is wet by the frit, which in turn holds the conductive metal in intimate contact with the cell's front surface. After firing, the oxide layer must be treated and removed in order to minimize series resistance.

There are several methods for removing the oxide layer. These include chemical treatment, an electrical discharge that breaks down the oxide barriers, and boiling water immersion. The chemical treatment consists of a short soak in dilute hydrofluoric acid or preferably ammonium bifluoride, which leaves less residue that might be humidity sensitive. The electrical method utilizes a capacitative discharge through the oxide barrier from the contact to the underlying silicon. The boiling water immersion, while the most simple, is not too effective. None of these techniques are very satisfactory. While good fill factors may be achieved, the results are not very consistent and the resulting cells are somewhat humidity sensitive. Generally, the cells revert to their original curve shape after humidity exposure.

In view of the problems with humidity, it became necessary to develop a firing technique for available contact materials that yielded good curve shape without subsequent operations.

3.8 FRONT METALLIZATIONS

Five categories of silver conductor metallization were screened for their suitability as the front contact metallization. These categories were commercially available, modified conductor compositions, modified frit conductors, diluted and modified frit conductors and customized frit conductors.

Among the large variety of commercial products tested, six produced a fair I-V curve shape. (Table 4).

Table 4

FAIR COMMERCIALLY AVAILABLE MATERIALS

1. E.I. Dupont 7095
2. EMCA Ag 92
3. ESL Type 590
4. Engelhard A2921 Mod. 025 (no longer available but may be obtained by diluting their E439A)
5. Thick Film Systems A256-a 50/50 blend of their standard 3345 and fritless silver A250
6. Transene 50

The optimal firing time and temperature for the above six materials is about twenty seconds at 700°C. Both Dupont 7095 and Transene 50 were eliminated from further tests because of the lack of firing consistency and series resistance problems, respectively.

The second category of front metallizations tested was the modified conductor composition. Four modified compositions were tried:

1. Elemental antimony added to TFS A256
2. Elemental antimony added to ESL Type 590
3. Powered bismuth added to Dupont 7095
4. Titanium Hydride added to Dupont 7095

Elemental antimony was added in the first two cases in the hope that the low temperature antimony - silver eutectic (440°C) would help to eliminate the series resistance problems previously encountered, and induce a deep junction at the metallization site. No improvement over previous compositions was realized.

In the third case powdered bismuth was added to the Dupont 7095. This resulted in a catastrophic loss of curve shape due to excessive shunting and was extremely sensitive to the firing temperature.

The final modification of a titanium hydride added to Dupont 7095 was tested because it was thought that after decomposition of the titanium hydride at a relatively low temperature, the hydrogen, in its atomic state would break down the oxide on the silicon surface and facilitate metal-silicon bonds. The decomposition of titanium hydride is slow up to 350°C, then begins to accelerate in the range of 350-450°C. Between 450°C and 650°C almost all of the hydride will be decomposed. This modification, however, did nothing to improve the characteristics of the fired paste. Even when the hydride was applied directly on top of the diffusion glass, the results were still negative. Ohmic contact through an oxide glass appears to be an insoluble problem with this composition, however, it appears that spin-on diffusion sources can be fired in nitrogen to yield an N^+ region and a surface silicon nitride. This nitride serves as a reasonably good AR coating and can be contacted directly without excessive series resistance.

The third category of the silver conductor metallizations is the modified frit conductors. The frit conductors used had phosphorus and antimony oxides added to the standard frit conductors. This was done to aid in the prevention of junction shunting and to decrease the sensitivity to changes in the firing time and temperature. The use of antimony in the frit composition was thought to be especially advantageous, because of the potential for oxidation-reduction reactions at the silicon surface. Both the phosphorus and antimony oxides used in the frit composition came from standard spray-on diffusion sources. The use of both of these oxides resulted in a definite improvement on the paste performance in both the prevention of junction shunting and the

decrease of sensitivity to changes in the firing time and temperature. The most effective materials tested were Transene n-diffusol and Emulsitone #773 (Antimony source). The following formulations performed well:

a. E.I. DuPont 7095 + Emulsitone #773
b. E.I. DuPont 7095 + Transene n-diffusol
c. ESL Type 590 + Emulsitone #773
d. ESL Type 590 + Transene n-diffusol
e. TFS A256 + Transene n-diffusol

The fourth category of silver conductor metallizations is the diluted and modified frit conductors. Cermalloy 4450, one of the commercial materials that was judged unsatisfactory, was diluted to one half the original frit content and modified with Emulsitone #773. Prior to dilution, the curve shape was plagued by high series resistance. After dilution modification by addition of the Emulsitone source, firing characteristics similar to those observed for the DuPont 7095 resulted.

The fifth and final of the silver conductor metallizations looked at were the customized frit conductors. A glass with a low fusion temperature, that had been used in another program as an insulator, was used as the frit. This frit had the following mole percent composition of the following elements:

Na_2O	14.2
Li_2O	4.3
NaF	10.0
P_2O_5	5.7
B_2O_3	42.9
SiO_2	22.9

This frit was found to be equivalent to some of the best commercially available products. It also had an excellent tolerance for firing time variations.

After the tests were completed on the front paste metallizations that were developed in the above five categories, a selection was made of the most promising front paste materials. A small lot of cells was made using these selections. The results of this test are presented in Table 5. All firings were done in an artificial air atmosphere with a coarse screen pattern. Both Thick Film System A256 + 2% n-diffusol and ESL Type 590 + 2% n-diffusol appear to show the best performance. TSF A256 with Transene n-diffusol was selected for the front contact paste material, because of its thixotropic properties. The components of the thick film system paste remain in solution, therefore giving the paste a long shelf life. The paste also turns into spreadable liquid when exposed to isothermal shearing stress.

3.9 MINIMUM CELL THICKNESS

The limiting factor in using screen printed contacts with thin cells is the warpage caused by the expansion differential between aluminum and silicon. Cells as thin as 2½ to 3½ mils can be manufactured with acceptable yields, however, these cells had a slight curvature. Cells which are 1½ to 2½ mils thick may be printed without breakage, but the firing frequently results in wafer fracture unless the perimeter is reinforced with greater silicon thickness.

3.10 DIELECTRIC ISOLATION

Five commercially available dielectric pastes were tested during the program. One of these pastes was selected for use on the wraparound cell configuration. The pastes tested were Thick Film Systems 1126RCB, 1126 1124, Electro Science Labs Type M-4023-B and Transene Type 980. All of the pastes were screened onto the back surface field side of the wafers using an actual production size screen. The wafers were separated into two

Table 5

Comparison of Front Paste Metallizations

Paste	Firing Time, sec.	Firing Temp., °C	I_{500} mA	Scatter in I_{500}, mA	I_{500} after 10 day, 80°C Humidity Test	#810 Post Humidity Tape Test
Engelhard A2921	15	700	92	29	90	pass
TSF A256	40	650	107	6	110	pass
	15	700	107	3	110	pass
	10	750	107	7	109	pass
ESL Type 590	30	650	105	11	99	pass
	15	700	104	6	107	pass
DuPont 7095 + 2% n-diffusol	40	650	99	11	107	pass
	15	700	104	7	105	pass
	10	750	107	4	108	pass
ESL Type 590 + 2% Emulsitone 733	30	650	104	5	100	pass
	15	700	105	6	105	pass
	10	750	105	6	107	pass
ESL Type 590 + 2% n-diffusol	50	650	102	7	107	pass
	20	700	112	3	113	pass
	15	750	107	7	110	pass
EMCA Ag 92	30	650	108	6	98	fail
	15	700	110	5	109	fail
	10	750	110	3	110	pass
DuPont 7095 + 2% Emulsitone #733	30	650	105	8	107	pass
	15	700	99	9	104	pass
TFS A256 + 2% n-diffusol	30	650	105	9	105	pass
	20	700	112	3	113	pass
	10	750	111	5	113	pass

groups, one for single printing and firing and the other for double printing and firing. The ideal printing method used the following sequence: (1) print on dielectric paste, (2) allow the paste to level for 10 minutes, (3) dry for ten minutes at 125°C, (4) fire in air for 5 minutes over a temperature range of 550°C-650°C, and (5) repeat steps one through four for those wafers that will be run through the process twice. After the firing was completed, a conductive silver epoxy was applied to the dielectric surface for isolation measurements. Table 6 is a compilation of electrical measurements for each paste and firing temperature.

The Thick Film Systems 1126RCB paste appears to be superior to the others tested. Although both the single and double printing and firing tested good at 550°C for both types of Thick Film Systems 1126, double coatings are preferable for filling in pinholes and eliminating shunting effects.

3.11 PROCESS SEQUENCE USED FOR NON-WRAPAROUND CELLS

The process sequence shown in Figure 1 has been developed during this contract. All process steps have been optimized and simplified using the information gathered during this program.

In view of the program's success in researching the back etch step, work was completed to see if the front etch step that removes the phosphorus glass layer on the surface could similarly be investigated.

Normally, prior to screen printing the front contact pattern, the phosphorus glass layer, grown during the diffusion, is removed by etching in a dilute solution of hydrofluoric acid. It was thought that if the glass frit in the paste could wet the phosphorus

Table 6

Dielectric Isolation Measurements

Single Printing

	°C				
	550	575	600	625	650
TFS 1126 RCB	G	GB	GB	B	GB
ESL Type M 4023-B	GB	GB	GB	GB	GB
Transene Type 980	B	B	B	B	B
TFS 1126	G	GB	GB	GB	B
TFS 1124	B	B	B	B	B
Double Printing					
TFS 1126 RCB	G	G	G	G	G
ESL Type M 4023-B	G	G	G	G	G
Transene Type 980	B	GB	GB	GB	GB
TFS 1126	G	G	G	G	G
TFS 1124	B	GB	GB	GB	G

G = Good (greater than 20 megohms)

B = Bad (less than 20 megohms)

GB = combination of good and bad

Each measured point is a minimum of 8 samples

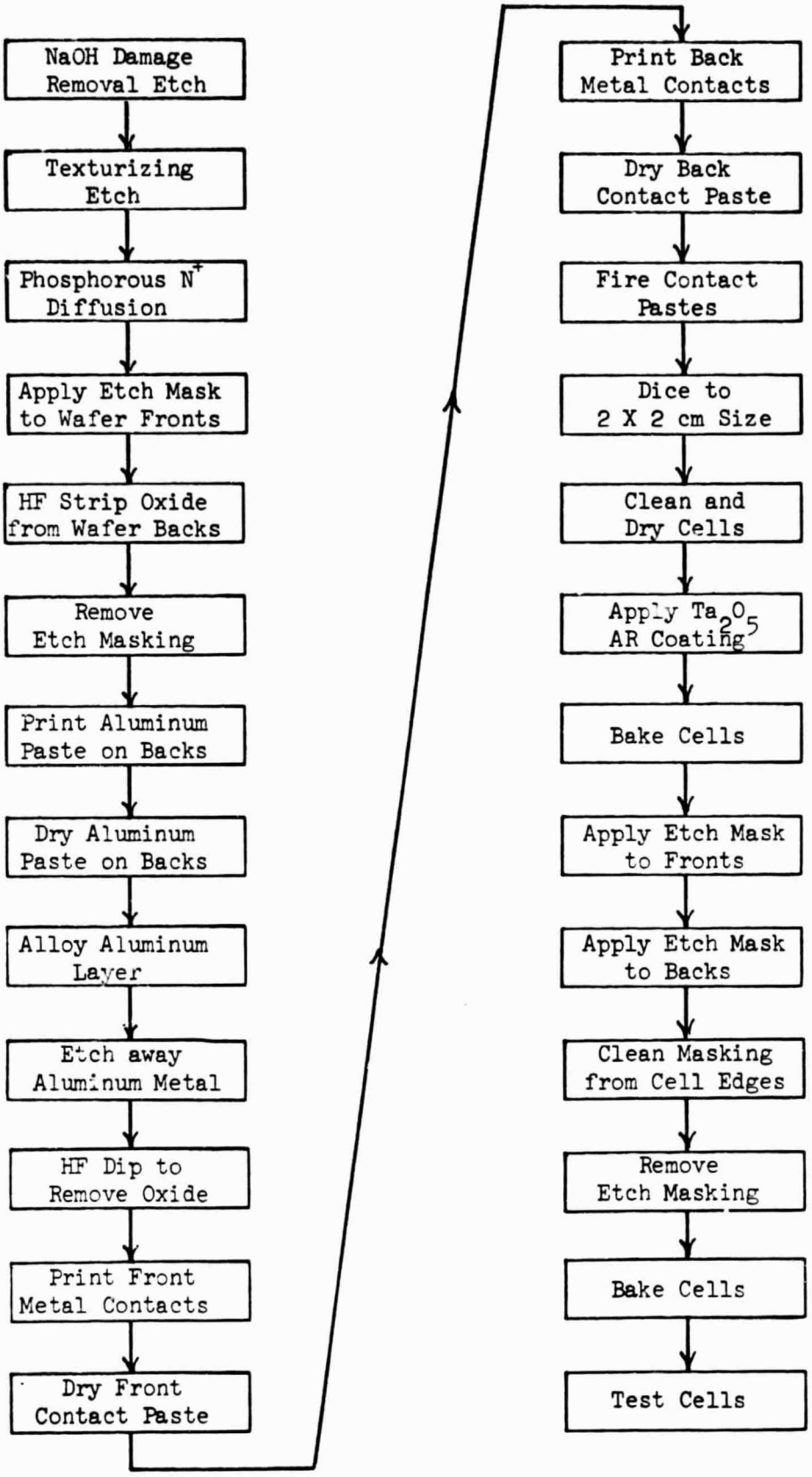

Figure 1

Process Sequence for Conventional (Non-Wraparound) Cells

glass layer and dissolve it into a solution, then the HF step could be eliminated. An experiment was performed to test this theory. Three groups of cells were screen printed with the front silver paste. In the first group, the glass layer was left untouched, the second group had the glass layer partially removed, and the third group had the glass layer completely removed. The experiment showed that the cells which were HF etched had better outputs, therefore showing that that this step could not be removed from the process sequence. The curve fill factors and open circuit voltages were also somewhat higher. The short circuit currents were satisfactory for all three groups. The group that was processed with the glass layer left intact had a higher series resistance. Firing of the silver paste was done at 700^{o}C in air. Twenty seconds was found to be the optimum time to produce good fill factors. Table 7 lists the average output values found for each group for a 20 second firing time.

This program also investigated the cause of the scatter in open circuit voltages found from time to time between lots in the process sequence of the paste back surface field supposedly processed in identical ways. One possible variation in the processing has been the cooling rate of wafers when they are removed from the aluminum alloying furnace. An experiment was designed to test the apparent effect of the cooling rate on the back surface field.

Identically diffused wafers were divided into two groups. One group was back etched prior to the aluminum paste BSF processing. The other group was processed without removing the diffused layer. Each of these groups was divided into three sub-groups to permit the use of three different dwell times during the alloying cycle. All cells were alloyed at 900^{o}C in artifical air. Ten, fifteen, and twenty seconds were used for the alloying times. Half of the wafers withdrawn from the furnace as rapidly as possible, and the other half withdrawn very slowly.

Table 7

HF REMOVAL OF PHOSPHOROUS GLASS LAYER

	V_{oc} (mV)	I_{sc} (mA)	I_{500} (mA)
Group 1 (no phosphorous glass removed)	598	140	116
Group 2 (partially removed)	603	136	122
Group 3 (completely removed)	604	141	127

The wafers were processed into 2 x 2 cm cells by etching away the metallic aluminum layer with hydrochloric acid, screen printing and firing a standard silver paste front grid pattern, dicing to size, and applying electron-beam evaporated Cr-Pd-Ag back contacts. It was found that the wafers which were not back-etched had markedly higher open circuit voltages when removed rapidly from the furnace, regardless of the dwell times. Wafers which had been back-etched exhibited higher values of V_{oc} for wafers that were removed slowly. The poorest V_{oc} values were found for non-back-etched wafers that were alloyed for twenty seconds and then withdrawn slowly. These data are shown below:

Group A (Back-Etched)

Dwell Time	Slow Removal Average V_{oc} (mV)	Fast Removal Average V_{oc} (mV)
10 sec.	578	584
15 sec.	594	577
20 sec.	593	576

Group B (Non-Back-Etched)

Dwell Time	Slow Removal Average V_{oc} (mV)	Fast Removal Average V_{oc} (mV)
10 sec.	573	602
15 sec.	595	600
20 sec.	566	600

A fast removal of the wafers has been incorporated into process sequence because of the results obtained in the experiment.

Work was also completed on refinement of the acid etch step to remove the excess aluminum from the back surface. A comparison was made between hydrochloric acid and sodium hydroxide treatment. Completed HCl etched cells showed a loss in V_{oc} indicating that some of the back surface field effect was lost. The cell output at the maximum load point was low and very poor fill factors were found.

Cells that received the NaOH treatment were better in V_{oc} and CFF. Figure 2 is the curve obtained for a NaOH treated cell. Series resistance was measured and a typcial result is shown in Figure 3. This value is still somewhat high, but is better than previous values obtained.

3.12 TEST RESULTS FOR NON-WRAPAROUND CELLS

One hundred conventional (non-wraparound) cells were fabricated using the process sequence developed under this program. The cells were fabricated using starting wafers that were approximately 57 mm in diameter. Two 20 x 20 mm cells were potentially possible from each wafer. The process sequence, along with the yield for each operation is shown in Table 8. The mechanical yield going into the electrical testing was 82%. After electrical testing 50% of the cells were over 13% efficient. The cells obtained from this lot provided sufficient quantities for delivery to the NASA-Lewis Research Center, as well as the quantities required for the environmental tests that were required.

A group of thirty cells was randomly selected for the electrical performance tests from the finished cells. These cells were assigned serial numbers one through thirty. The cells were tested electrically in simulated AMO sunlight using a Spectrosun® Mark III Solar Simulator. The cells were tested at a test block temperature of 28°C. The simulator was adjusted to the proper intensity level using a Standard Cell (No. 1037). Every sixth cell was tested for series resistance. Table 9 presents the electrical performance data and the average values for all thirty cells. Figure 4 and Figure 5 give the I-V plots for a representative cell (No. 6). These plots were used to establish the cell performance and the series resistance. After these performance tests, the thirty cells were boxed and shipped to the Project Manager at NASA-Lewis Research Center.

Figure 2

I-V Characteristics for Sodium Hydroxide Etched Cell

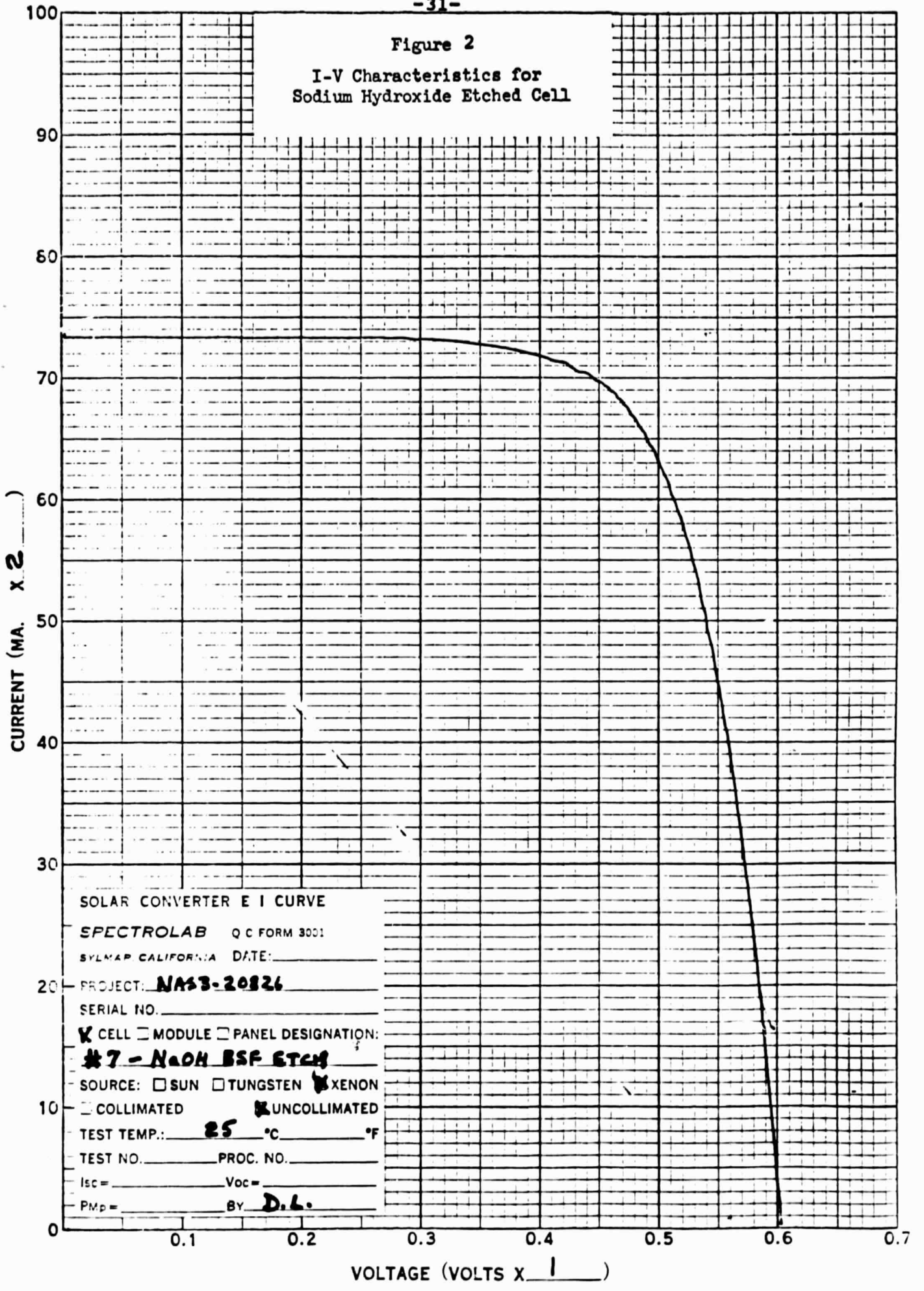

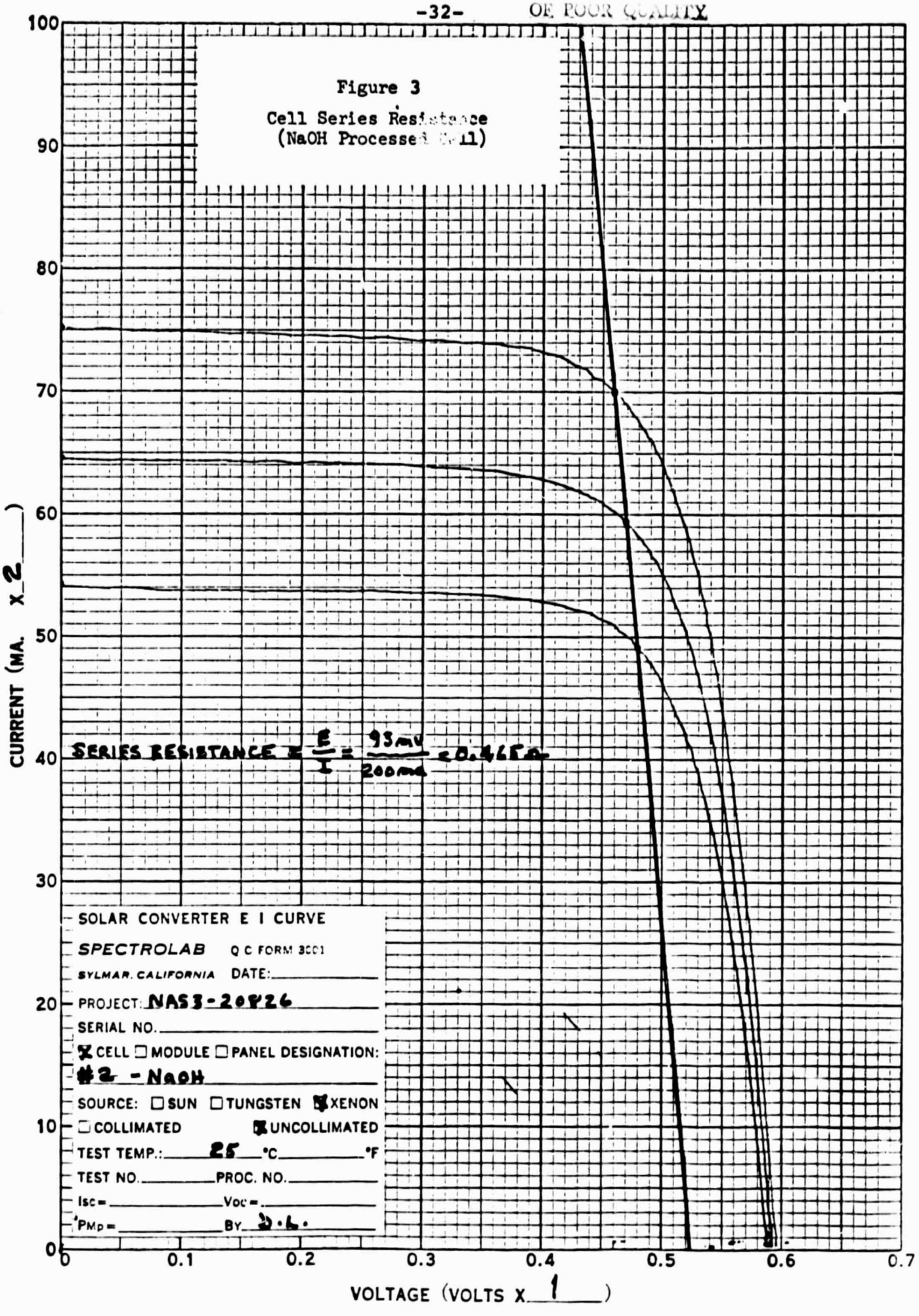

Table 8

PROCESS SEQUENCE SHOWING YIELDS AND LOSSES

Step No.	Operation	Qty In	Qty Out	% Yield	Loss Due To
1	Damage Removal Etch	100	100	100.0	
2	Texturizing Etch	100	95	95.0	Mechanical breakage
3	N^+ Diffusion	95	95	100.0	
4	Mask Wafer Fronts	95	95	100.0	
5	Oxide Strip Backs	95	94	98.9	Mechanical breakage
6	Remove Masking	94	94	100.0	
7	Print Aluminum Paste	94	94	100.0	
8	Dry Paste	94	94	100.0	
9	Alloy Aluminum	94	93	98.9	Mechanical breakage
10	Aluminum Etch	93	93	100.0	
11	HF Dip	93	93	100.0	
12	Print Front Metal	93	93	100.0	
13	Dry Front Paste	93	93	100.0	
14	Print Back Metal	93	93	100.0	
15	Dry Back Paste	93	93	100.0	
16	Fire Metal Pastes	93	93	100.0	
17	Dice to Size	93	186	100.0	
18	Clean and Dry	186	186	100.0	
19	Apply AR Coating	186	182	97.8	Mechanical breakage
20	Bake Cells	182	182	100.0	
21	Mask Cell Fronts	182	182	100.0	
22	Mask Cell Backs	182	182	100.0	
23	Clean Cell Edges	182	182	100.0	
24	Etch Edges	182	182	100.0	
25	Remove Masking	182	164	90.1	Mechanical Breakage
26	Bake Cells	164	164	100.0	
27	Electrical Test	164			

Table 9

ELECTRICAL PERFORMANCE TEST DATA FOR NON-WRAPAROUND CELLS
(AMO Illumination at 28°C)

Cell No.	V_{oc} (mV)	I_{sc} (mA)	P_{max} (mW/cm^2)	Calc. Eff.(%)	Calc. CFF	R_{series} (ohms)
1	590	157	17.90	13.2	.77	----
2	590	159	18.04	13.3	.77	----
3	591	158	17.82	13.2	.76	----
4	594	164	17.70	13.1	.73	----
5	590	157	17.95	13.3	.77	----
6	591	160	17.81	13.2	.75	0.19
7	591	157	17.86	13.2	.77	----
8	591	158	17.70	13.1	.76	----
9	591	158	17.73	13.1	.76	----
10	594	167	17.95	13.3	.72	----
11	594	164	18.17	13.4	.75	----
12	594	165	18.08	13.4	.74	0.36
13	592	159	18.00	13.3	.77	----
14	592	160	17.85	13.2	.75	----
15	591	157	17.46	12.9	.75	----
16	590	167	17.87	13.2	.73	----
17	591	158	18.03	13.3	.77	----
18	590	159	18.13	13.4	.77	0.20
19	591	157	17.98	13.3	.7o	----
20	592	158	18.01	13.3	.77	----
21	590	156	17.82	13.2	.77	----
22	592	157	17.93	13.3	.77	----
23	591	160	17.69	13.1	.75	----
24	592	158	18.25	13.5	.78	0.18
25	595	162	18.00	13.3	.75	----
26	592	162	18.15	13.4	.76	----
27	593	159	18.07	13.4	.77	----
28	591	159	18.04	13.3	.77	----
29	593	160	17.91	13.2	.75	----
30	591	164	18.12	13.4	.75	0.25
Av.	591.7	159.9	17.93	13.3	.759	0.236 (5 cells)

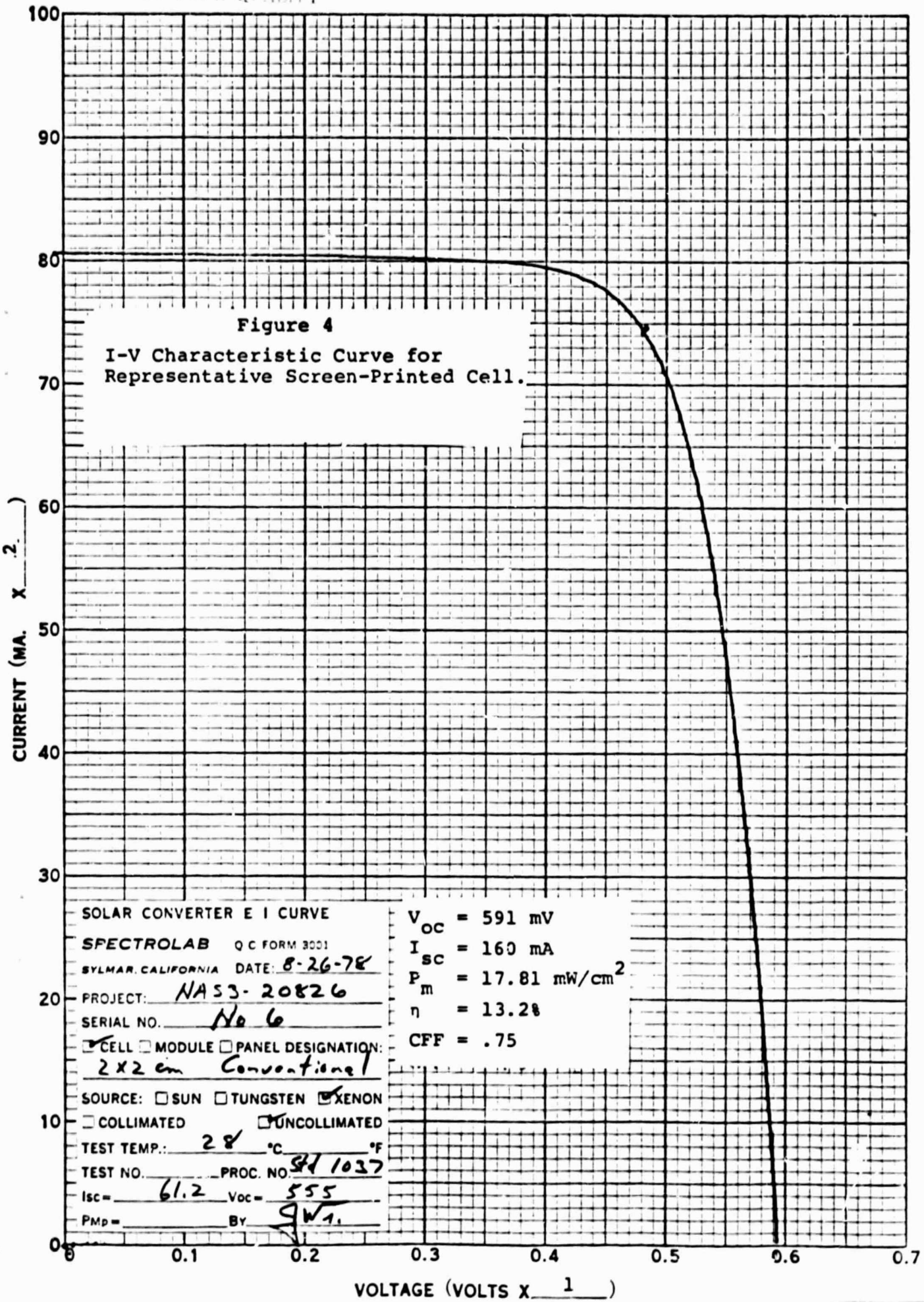

Figure 4

I-V Characteristic Curve for Representative Screen-Printed Cell.

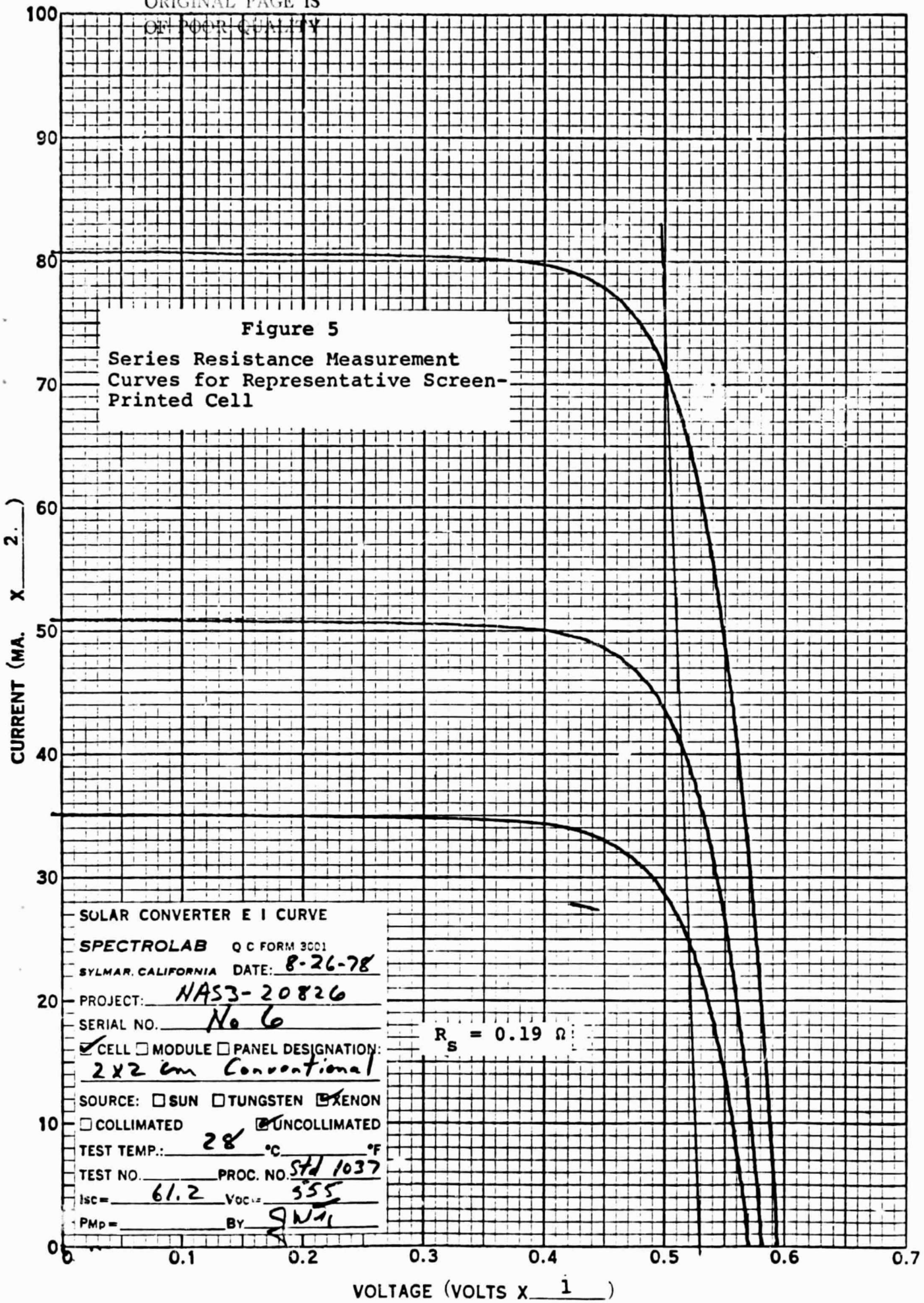

Figure 5

Series Resistance Measurement Curves for Representative Screen-Printed Cell

Ten cells were randomly selected from the f
inclusion in the boiling water tests. The ted
for electrical performance at AMO and 28°
immersed in boiling deionized water for by
a one minute bake on a hot plate at app nd
tested again at AMO and 28°C. The elect ed
before and after the boiling water treatme d in
Table 10. Unexpectedly all ten cells disp vement
in output power and curve shape after the b The
cells were then passed through a standard ta esting machine
using Scotch Brand #600 tape. There was no of loss of
the AR coating or front metallization, how dentifying
penciled numbers were removed from the ce he tape.
A representative before and after I-V se is shown
in Figure 6. The cells were boxed and s the Project
Manager at NASA-Lewis Research Center.

Twelve randomly selected cells were se or inclusion in
the high temperature and high humidit These cells were
tested under a solar simulator at 28° I-V curves were
plotted for each cell. The cells we n boiling D.I.
water for ten minutes, baked on a h r one minute at
approximately 375°C and tested aga cells were placed
in a chamber at 80°C and 90% (min ve humidity for a
period of ten days, after which e tested within a few
hours of removal from the chamber without any attempt to dry
them.

The cells were then given a one minute bake on a hot plate at 375°C and tested again. Unfortunately these tests cannot be compared with the three earlier tests, since routine maintenance had been performed on the simulator, resulting in a slight change in the red/blue ratio of the source. The curve fill factors, however, can be compared since they are not spectrum dependent.

Table 10

ELECTRICAL PERFORMANCE BEFORE AND AFTER 10 MIN. BOILING WATER IMMERSION

Cell No.	V_{oc} (mV)		I_{sc} (mA)		P_{max} (mW/cm^2)		Calc. Eff.		Calc. CFF	
	Before	After	Before	After	Before	After	Before	After	Before	After
B-01	591	592	157	158	16.97	17.76	12.5	13.1	.73	.76
B-02	591	592	159	162	16.93	17.78	12.5	13.1	.72	.74
B-03	594	594	156	157	17.40	18.14	12.9	13.4	.75	.77
B-05	592	592	156	157	16.49	17.82	12.2	13.2	.71	.76
B-07	591	592	154	156	15.68	17.72	11.6	13.1	.68	.76
B-09	590	591	154	156	17.19	17.85	12.7	13.2	.75	.77
B-12	591	591	155	156	16.82	17.84	12.4	13.2	.73	.77
B-16	591	595	161	163	16.89	18.74	12.5	13.9	.71	.77
B-21	592	594	158	160	16.79	18.31	12.4	13.5	.71	.77
B-23	591	592	152	154	16.27	17.55	12.0	13.0	.72	.77

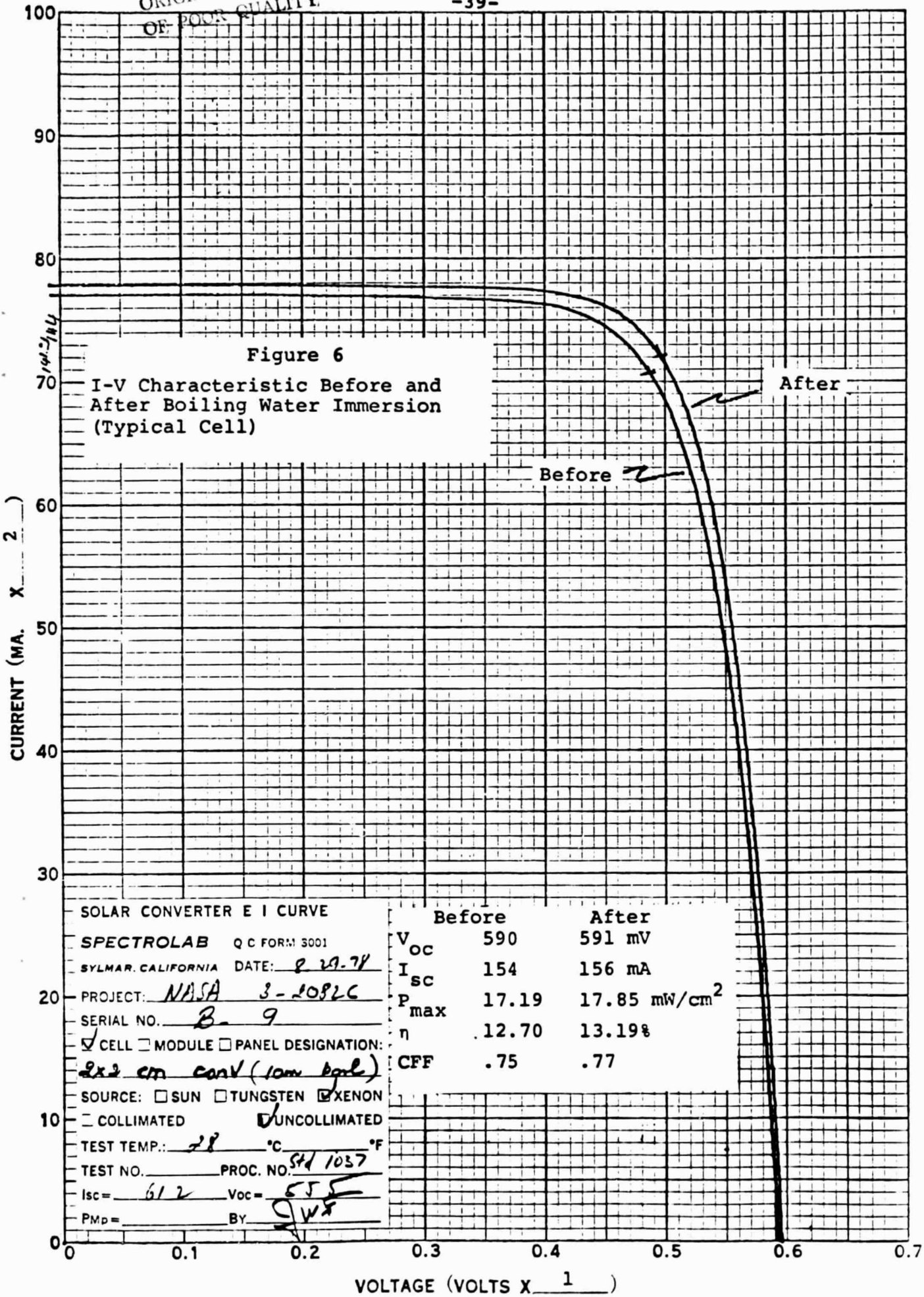

Figure 6

I-V Characteristic Before and After Boiling Water Immersion (Typical Cell)

	Before	After
V_{oc}	590	591 mV
I_{sc}	154	156 mA
P_{max}	17.19	17.85 mW/cm^2
η	12.70	13.19%
CFF	.75	.77

The changes noted here can be attributed to the one minute bake on the hot plate after the humidity tests. The cells were subjected to the water boil and bake treatment and tested again. These data are presented in Table 11. The point where the simulator was cleaned is indicated by a dashed line in the "Test Condition" column. Figures 7 and 8 are typical I-V curves for a single cell. All cells exhibited an improvement in curve shape after the first boil/bake cycle. After the temperature-humidity chamber test, all cells had improved short circuit currents, little or no change in open circuit voltage and a degradation in curve fill factor. The second boil/bake cycle yielded little change in performance from that found after the cells had been baked following removal from the temperature-humidity chamber. It should be noted that all values of V_{oc} and I_{sc} were measured using a digital volt meter readout, rather than obtaining these values from the I-V curves themselves.

After all electrical testing was complete, all cells were tape peel tested using Scotch brand #600 tape in a conventional tape test machine. One cell was broken during these tests, but the front contact metallization of all cells appeared to be unaffected by the temperature-humidity storage and the repeated boil/bake cycles. Back contacts appeared to have a slightly more "pepper and salt" look after the tape peel test, however, no obvious metallization was removed by the tape, even though the tape removed the identifying pencil number from the backs of the cells.

To assure that the scatter in cell performance was actually the result of cell variation and not caused by test fixture contact problems, the following test was performed. One cell was chosen at random from the completely finished lot. This cell had not been screen tested. Three I-V curves were taken of this cell. The cell was taken completely out of the test fixture and

Table 11

Temperature - Humidity Test Data

Cell No.	Test Condition	V_{oc} (mV)	I_{sc} (mA)	P_{max} (mW/cm^2)	Calc. Eff.(%)	Calc. FF
01	Initial Test	592	159	17.16	12.7	.73
	Post Boil/Bake	595	160	18.44	13.6	.77
	Post Temp/Humidity	593	165	17.41	12.9	.71
	Pre-Boil/Bake	594	166	18.25	13.5	.74
	Post Boil/Bake	594	164	17.94	13.3	.74
02	Initial Test	590	156	15.40	11.4	.67
	Post Boil/Bake	591	156	16.85	12.5	.73
	Post Temp/Humidity	589	161	15.53	11.5	.66
	Pre-Boil/Bake	592	161	16.60	12.3	.70
	Post Boil/Bake	593	160	16.33	12.1	.69
03	Initial Test	592	159	17.64	13.0	.75
	Post Boil/Bake	593	160	18.25	13.5	.77
	Post Temp/Humidity	592	165	17.88	13.2	.73
	Pre-Boil/Bake	593	164	17.78	13.1	.73
	Post Boil/Bake	593	164	17.78	13.1	.73
04	Initial Test	586	154	15.81	11.7	.70
	Post Boil/Bake	589	155	17.03	12.6	.75
	Post Temp/Humidity	588	160	16.04	11.9	.68
	Pre-Boil/Bake	591	159	18.41	13.6	.78
	Post Boil/Bake	591	158	18.41	13.6	.79
05	Initial Test	590	153	16.26	12.0	.72
	Post Boil/Bake	592	154	16.99	12.6	.75
	Post Temp/Humidity	590	161	16.26	12.0	.68
	Pre-Boil/Bake	594	157	16.51	12.2	.71
	Post Boil/Bake	593	156	16.51	12.2	.71
06	Initial Test	590	157	17.37	12.8	.75
	Post Boil/Bake	592	158	18.12	13.4	.77
	Post Temp/Humidity	591	163	17.37	12.8	.72
	Pre-Boil/Bake	593	162	18.05	13.3	.75
	Post Boil/Bake	592	162	17.81	13.2	.74
07	Initial Test	589	155	16.91	12.5	.74
	Post Boil/Bake	592	156	17.80	13.2	.77
	Post Temp/Humidity	589	161	16.57	12.2	.70
	Pre-Boil/Bake	593	159	17.64	13.0	.75
	Post Boil/Bake	592	159	17.43	12.9	.74
08	Initial Test	591	156	15.75	11.6	.68
	Post Boil/Bake	591	157	17.17	12.7	.74
	Post Temp/Humidity	590	162	15.19	11.2	.64
	Pre-Boil/Bake	594	161	16.01	11.8	.67
	Post Boil/Bake	593	160	16.49	12.2	.70

Table 11 (cont'd)

Temperature - Humidity Test Data

Cell No.	Test Condition	V_{oc} (mV)	I_{sc} (mA)	P_{max} (mW/cm^2)	Calc. Eff.(%)	Calc. FF
09	Initial Test	589	160	17.16	12.7	.73
	Post Boil/Bake	592	162	18.25	13.5	.76
	Post Temp/Humidity	590	164	16.46	12.2	.68
	Pre-Boil/Bake	594	164	17.84	13.2	.73
	Post Boil/Bake	593	164	17.84	13.2	.73
10	Initial Test	582	153	14.63	10.8	.66
	Post Boil/Bake	585	154	16.03	11.8	.71
	Post Temp/Humidity	585	158	14.84	11.0	.64
	Pre-Boil/Bake	588	157	15.52	11.5	.67
	Post Boil/Bake	588	157	15.52	11.5	.67
11	Initial Test	593	162	17.08	12.6	.71
	Post Boil/Bake	595	164	19.05	14.1	.78
	Post Temp/Humidity	593	168	17.28	12.8	.69
	Pre-Boil/Bake	595	166	17.22	12.7	.70
	Post Boil/Bake	592	166	17.22	12.7	.70
12	Initial Test	589	150	15.87	11.7	.72
	Post Boil/Bake	589	153	16.98	12.5	.75
	Post Temp/Humidity	589	156	15.87	11.7	.69
	Pre-Boil/Bake	592	156	16.10	11.9	.70
	Post Boil/Bake	592	154	16.35	12.1	.72
Av.	Initial Test	589	156	16.42	12.1	.71
	Post Boil/Bake	591	157	17.58	13.0	.75
	Post Temp/Humidity	590	162	16.39	12.1	.69
	Pre-Boil/Bake	593	161	17.16	12.7	.72
	Post Boil/Bake	592	160	17.14	12.7	.72

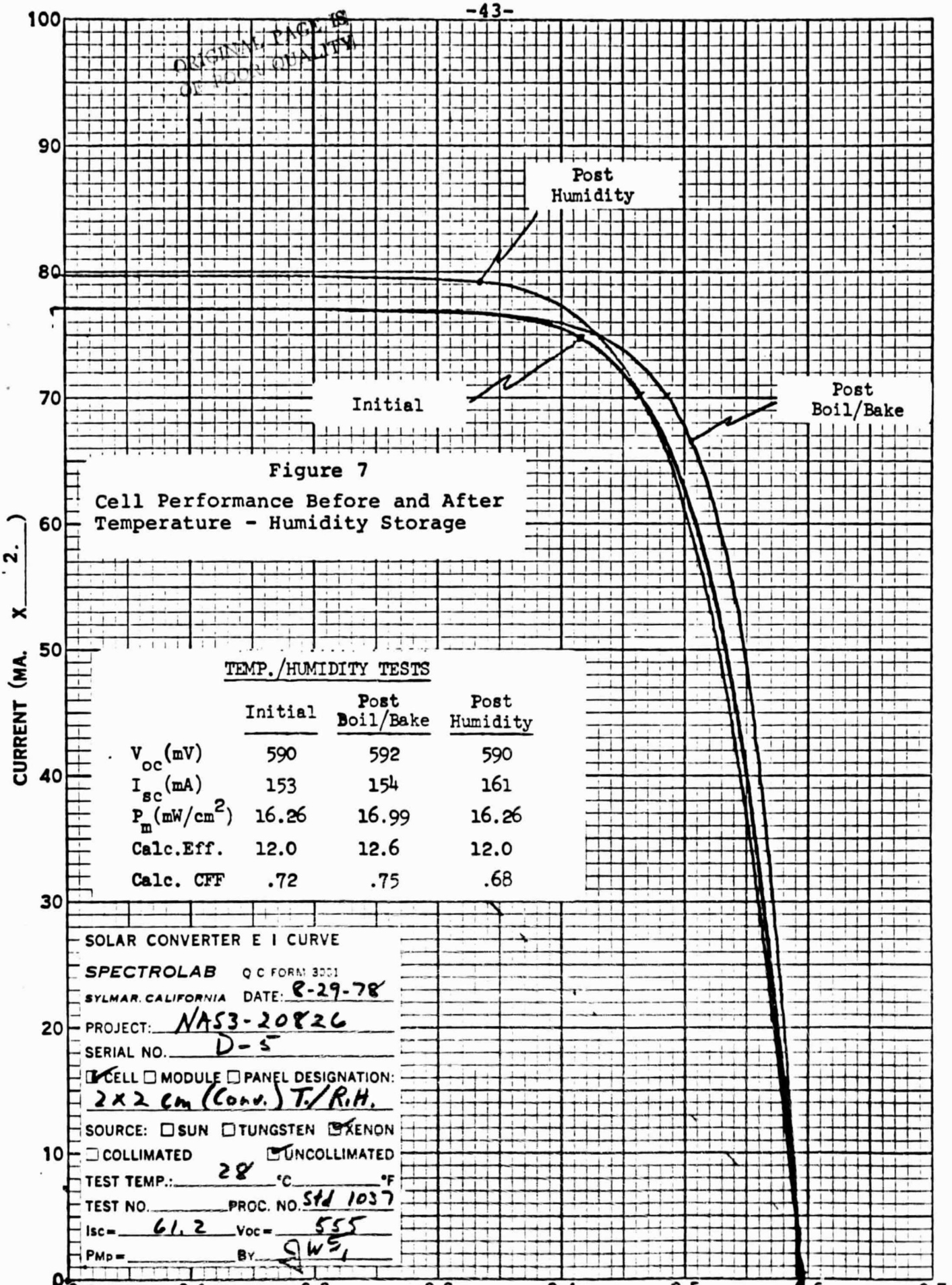

Figure 7

Cell Performance Before and After Temperature - Humidity Storage

TEMP./HUMIDITY TESTS

	Initial	Post Boil/Bake	Post Humidity
V_{oc} (mV)	590	592	590
I_{sc} (mA)	153	154	161
P_m (mW/cm^2)	16.26	16.99	16.26
Calc.Eff.	12.0	12.6	12.0
Calc. CFF	.72	.75	.68

SOLAR CONVERTER E I CURVE

SPECTROLAB Q C FORM 3001

SYLMAR, CALIFORNIA DATE: 8-29-78

PROJECT: NAS3-20826

SERIAL NO. D-5

☑ CELL ☐ MODULE ☐ PANEL DESIGNATION:

2 x 2 cm (Conv.) T/R.H.

SOURCE: ☐ SUN ☐ TUNGSTEN ☑ XENON

☐ COLLIMATED ☑ UNCOLLIMATED

TEST TEMP.: 28 °C ____ °F

TEST NO. ____ PROC. NO. Std 1037

Isc = 61.2 Voc = 555

PMp = ____ BY ____

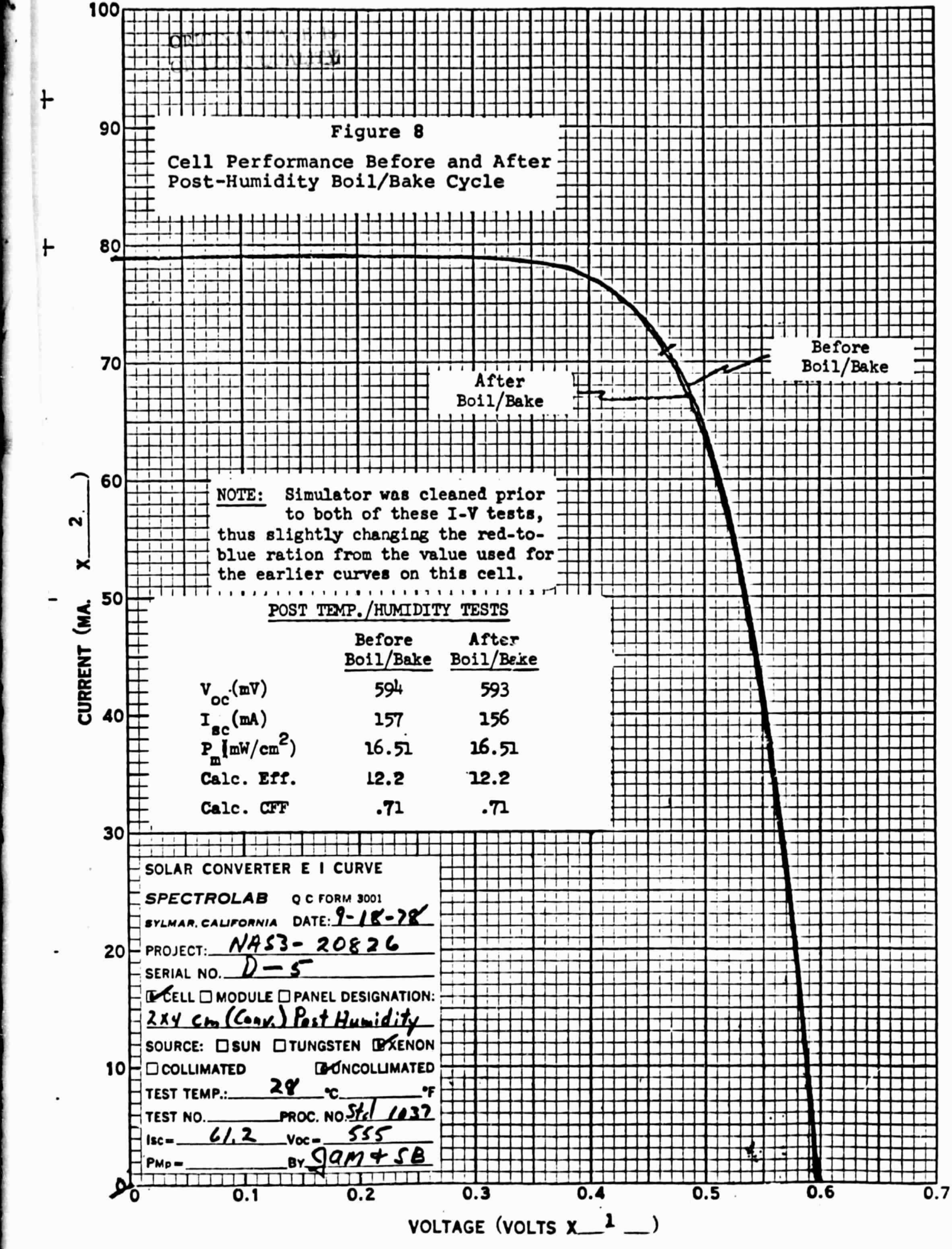
Figure 8
Cell Performance Before and After Post-Humidity Boil/Bake Cycle
Before Boil/Bake
After Boil/Bake
NOTE: Simulator was cleaned prior to both of these I-V tests, thus slightly changing the red-to-blue ration from the value used for the earlier curves on this cell.
POST TEMP./HUMIDITY TESTS
Before Boil/Bake
After Boil/Bake
V_{oc} (mV) 594 593
I_{sc} (mA) 157 156
P_m (mW/cm^2) 16.51 16.51
Calc. Eff. 12.2 12.2
Calc. CFF .71 .71
SOLAR CONVERTER E I CURVE
SPECTROLAB Q C FORM 3001
SYLMAR, CALIFORNIA DATE: 9-18-78
PROJECT: NAS3-20826
SERIAL NO. D-5
☑ CELL ☐ MODULE ☐ PANEL DESIGNATION:
2x4 cm (Conv.) Post Humidity
SOURCE: ☐ SUN ☐ TUNGSTEN ☑ XENON
☐ COLLIMATED ☑ UNCOLLIMATED
TEST TEMP.: 28 °C °F
TEST NO. PROC. NO. Std 1037
Isc = 61.2 Voc = 555
PMp = BY JAM + SB
CURRENT (MA. X 2)
VOLTAGE (VOLTS X 1)
100
90
80
70
60
50
40
30
20
10
0
0.1
0.2
0.3
0.4
0.5
0.6
0.7

replaced each time. The cell was retested three times again in a different fixture. The I-V curves for all six measurements were reproducible and identical. All of the cells used for the temperature-humidity test were shipped to the NASA-Lewis Program Manager.

Five cells were randomly selected for the thermal shock tests. I-V curves were made for each cell under a solar simulator at 28°C and AMO. The cells were loaded into a basket and immersed in the boiling water for thirty seconds. The cells were transferred over a period of sixty seconds to boiling D.I. water and immersed in the boiling water for thirty seconds. The cells were transferred back to the liquid nitrogen over a period of thirty seconds and immersed in the liquid nitrogen for thirty seconds. This cycle was repeated for fifteen times after which the cells were again tested electrically as before. The cells were tape peel tested using Scotch brand #600 tape. No contact failures were found, although the tape removed the identifying pencil numbers from the cell backs. The data obtained is listed in Table 12. These cells were also shipped to the NASA-Lewis Program Manager. It should be noted that these thermal shock tests were somewhat more severe than those required by the contract Statement of Work. Figure 9 shows a typical I-V curve obtained during these tests.

Tests were also completed on the measurement of the sheet resistance of the front contact metallization. Initially, an attempt was made to evaluate the sheet resistance with a four point probe technique, but the resistivity was too low to permit reliable readings. Therefore a printing screen was designed to allow measurement of the voltage drop over a long (72.0 cm) continuous 0.25 mm wide contact printed on a 2 inch round silicon wafer. The Cartesian coordinate diagram used for generating the test pattern is shown in Figure 10. This pattern was made up in two screen

Table 12

Thermal Shock Test Data

Cell No.	Test Condition	V_{oc} (mV)	I_{sc} (mA)	P_{max} (mW/cm^2)	Calc. Eff.(%)	Calc. FF
19	Before Thermal Shock	591	156	17.82	13.2	.77
19	After Thermal Shock	588	156	17.82	13.2	.78
20	Before Thermal Shock	591	159	16.45	12.2	.70
20	After Thermal Shock	591	159	16.96	12.5	.72
21	Before Thermal Shock	593	160	18.16	13.4	.77
21	After Thermal Shock	593	160	18.38	13.6	.77
22	Before Thermal Shock	592	160	17.73	13.1	.75
22	After Thermal Shock	592	160	18.19	13.4	.77
23	Before Thermal Shock	587	158	16.15	11.9	.70
23	After Thermal Shock	587	159	17.34	12.8	.74
Averages:						
	Before Thermal Shock	591	159	17.26	12.8	.74
	After Thermal Shock	590	159	17.74	13.1	.76

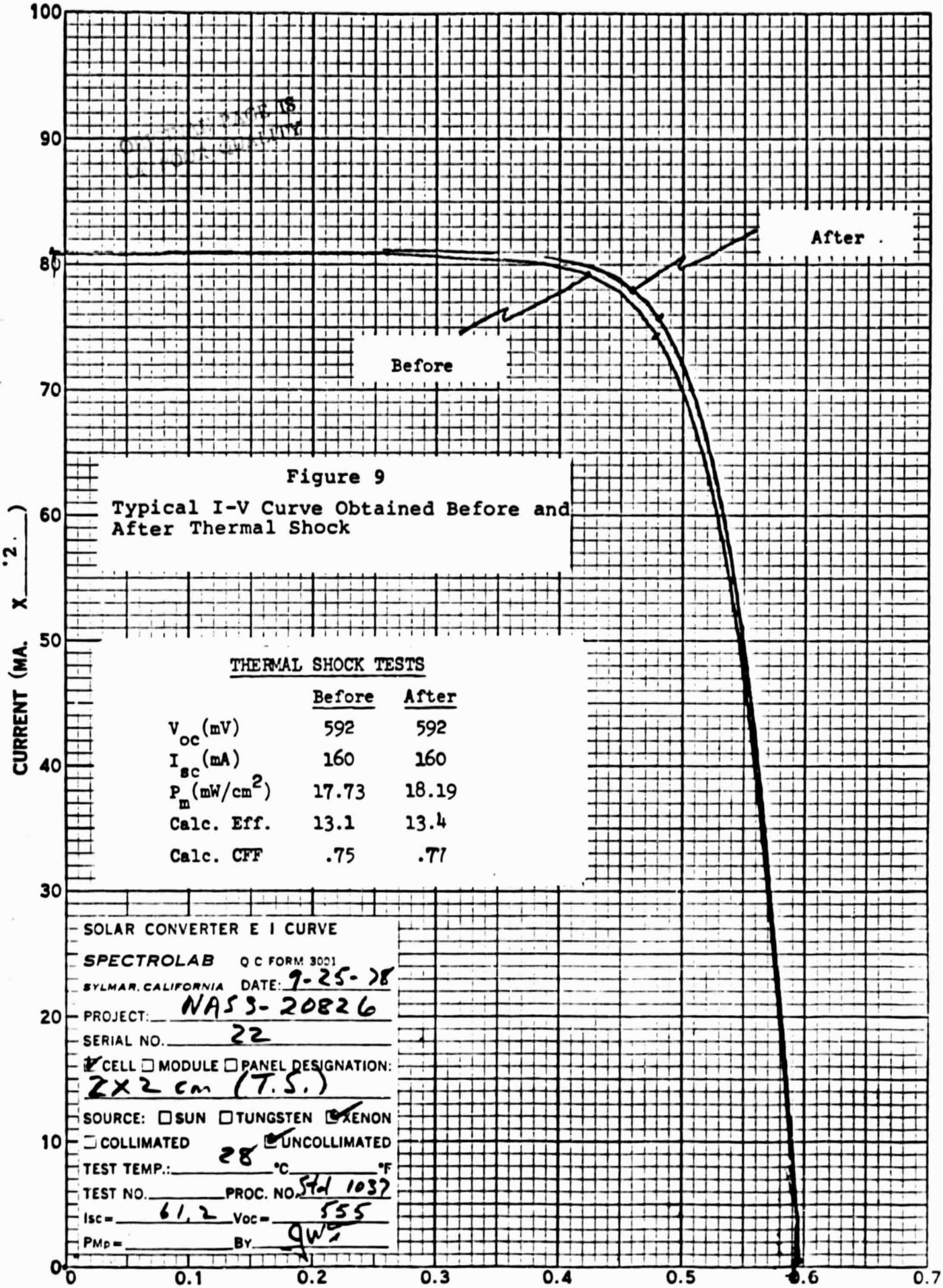

Figure 9

Typical I-V Curve Obtained Before and After Thermal Shock

THERMAL SHOCK TESTS

	Before	After
V_{oc} (mV)	592	592
I_{sc} (mA)	160	160
P_m (mW/cm^2)	17.73	18.19
Calc. Eff.	13.1	13.4
Calc. CFF	.75	.77

SOLAR CONVERTER E I CURVE
SPECTROLAB Q C FORM 3001
SYLMAR, CALIFORNIA DATE: 9-25-78
PROJECT: NAS3-20826
SERIAL NO. 22
☑ CELL ☐ MODULE ☐ PANEL DESIGNATION:
2X2 cm (T.S.)
SOURCE: ☐ SUN ☐ TUNGSTEN ☑ XENON
☐ COLLIMATED ☑ UNCOLLIMATED
TEST TEMP.: 28 °C °F
TEST NO. PROC. NO. Std 1037
Isc = 61.2 Voc = 555
PMp = BY QW

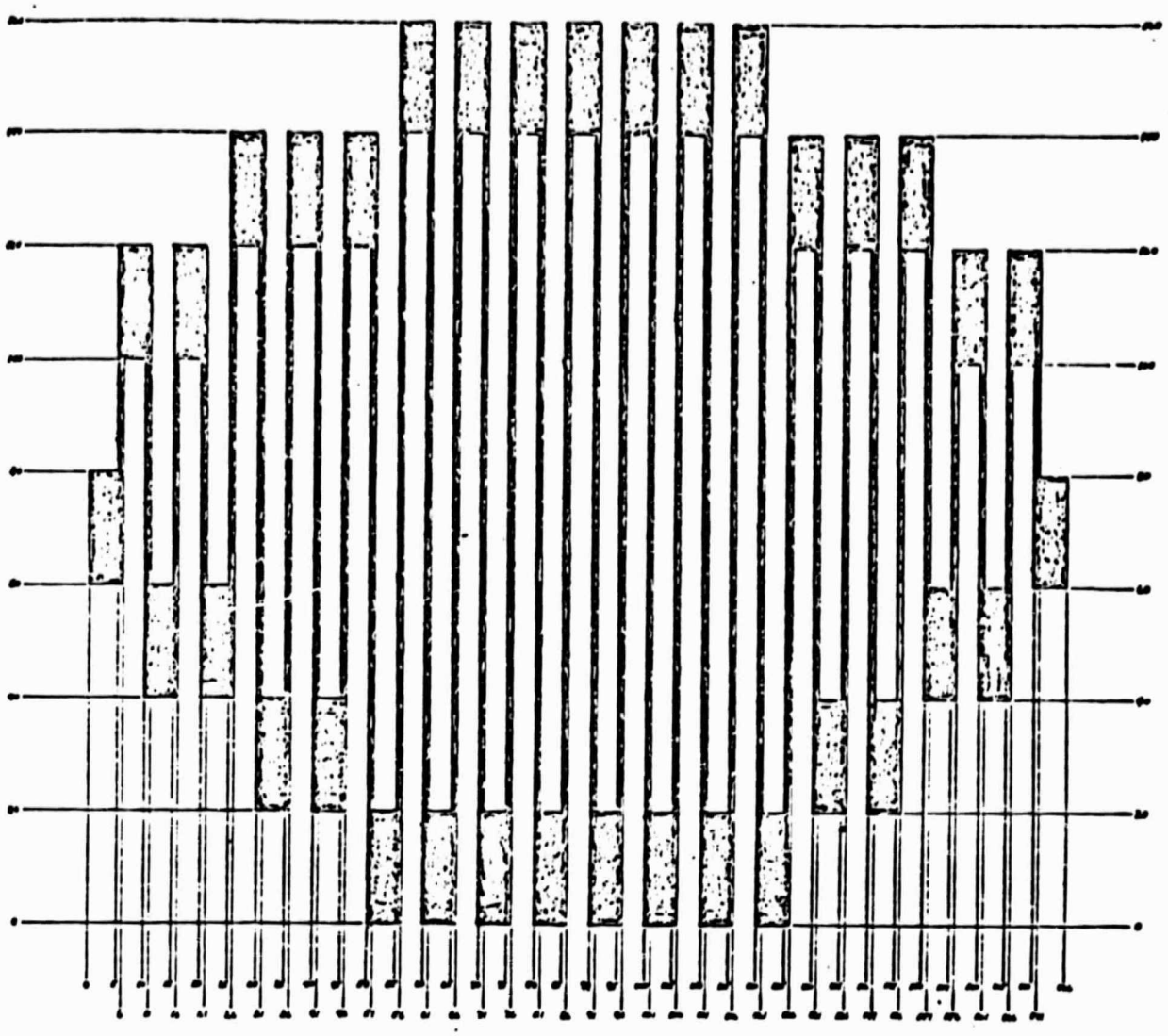

Figure 10

Cartesian Coordinate Diagram for
a Front Contact Metallization Test Pattern
(each division equals 0.25 mm)

mesh sizes (200 and 325) using a 22° screen orientation to minimize the possibility of wires in the screen coinciding with openings in the pattern.

A test metallization was printed on dummy silicon wafers that had been etched and texturized exactly the same as those used for solar cells. The paste used was identical to that found to give the best results to date for a screen printed solar cell, namely Thick Film Systems A256 with Transene n-diffusol added. The screen printed paste was dried for 15 minutes at 150°C and fired for 20 seconds at 700°C. Line thickness was established using a Taylor-Hobson Talysurf-4.

Current leads were soldered to the end tabs of the pattern and voltage leads to the adjacent inner tabs. Measurements of current and voltage, along with the physical dimensions gave average values of specific resistivity of 5 to 6 x 10^{-6} ohm-cm for the fired metallization. Because of time and funding, this investigation was not extended to include measurements of other paste systems or other drying and firing schedules.

3.13 PROCESS SEQUENCE USED FOR WRAPAROUND CONTACT CELLS

The process sequence used for the wraparound cell configuration is exactly the same as the conventional sequence shown in Figure 1 on page 26. After alloying the aluminum, however, the aluminum oxide powder was removed to reveal the metallic aluminum layer which was left in place. It was decided, because of immediate availability, to use the dielectric screens on hand for printing the wraparound isolation layer. The wafers were wax mounted on dummy silicon wafers and diced to 2 x 4 cm. This permits cutting clear through the wafers leaving a square edge which is better geometrically for wraparound printing than a scored and broken edge.

Two layers of Thick Film Systems #1125RCB dielectric glass were printed on the solar cell. Only the second layer wrapped around the cell's edge. The cells were then dried and fired in turn.

After ink masking all of the cell except the front face, the cells were etched in hydrofluoric acid to remove any possible oxide layers prior to applying the screen printed contacts. After removing the ink masking, the contact metallization was screen printed, applying first the front surface wraparound gridlines, drying them, printing on the back contact pads, drying them, and then firing both simultaneously. The contact paste used was the same as used on the conventional cells, namely Thick Film Systems A256 that had been doped with Transene n-diffusol solution. Lot Ø was printed using a gridline screen pattern that was on hand (it had been used on Contract No. NAS3-20029[4]), since the screens made up previously for this contract were found to have a design error. This older screen produced gridlines having a width of about 0.25 mm and had a density of three lines per centimeter. Redesigned screens were received in time for use on Lots 1 and 2, so the gridlines on these lots were about 0.13 to 0.15 mm wide and had a density of four lines per centimeter.

After firing the contacts, the cells were AR coated with Ta_2O_5 and then cut in half to yield two 2 x 2 cm cells. The cells were ink masked and edge etched. After stripping the ink masking, they were baked and tested.

3.14 TEST RESULTS FOR WRAPAROUND CELLS

Three lots of wafers were processed into 2 x 2 cm wraparound contact cells using the process developed under this program. Thick Film Systems #1126RCB dielectric glass was used for the isolation layer. The cells were screened for electrical performance at 28°C under AMO illumination. It was found that

while nearly all of the cells exhibited open circuit voltages and short circuit currents similar to those of the conventional cells processed earlier in the program, nearly all of the I-V curves were characterized by relatively low curve fill factors. Using a cutoff of 10% conversion efficiency, a group of cells was assembled from the three lots for shipment to the NASA-Lewis Research Center. Sixty-five percent of the cells had over ten percent efficiency. Cells were also assembled for the boiling water and thermal shock environmental testing. Table 13 presents the data for the 25 wraparound contact cells shipped. Tables 14 and 15 present the data for the boiling water and thermal shock tests, respectively. Those cells subjected to the environmental tests were tape peel tested with Scotch Brand #600 tape with no failures. No temperature humidity tests were undertaken because of the lack of time and funding.

Table 13

Data for Representative Screen Printed Wraparound Contact
2 X 2 cm Silicon Solar Cells With Dielectric Isolation

Cell No.	V_{oc} (mV)	I_{sc} (mA)	Max. Pwr. Density (mW/cm^2)	Calculated Efficiency	Calculated Curve Factor
Ø-01	596	178	15.99	11.30	.60
Ø-02	601	173	15.98	11.81	.61
Ø-07	591	168	15.04	11.11	.60
Ø-10	583	164	14.65	10.82	.58
Ø-13	595	167	15.14	11.19	.61
Ø-15	592	167	15.63	11.55	.63
Ø-16	592	168	16.89	12.48	.68
Ø-17	591	167	16.30	12.05	.66
Ø-18	592	170	14.82	10.95	.59
Ø-19	589	167	15.74	11.63	.64
Ø-20	589	168	14.58	10.77	.59
Ø-21	591	170	14.80	10.93	.59
Ø-27	588	168	14.61	10.80	.59
Ø-28	588	165	15.51	11.46	.64
1-08	587	171	15.44	11.41	.61
1-10	592	168	14.74	10.89	.59
1-11	592	172	15.91	11.76	.62
1-14	598	171	15.09	11.15	.59
1-15	589	168	14.78	10.92	.60
1-16	587	166	14.62	10.80	.60
2-01	592	161	15.50	11.45	.62
2-02	592	172	16.73	12.36	.67
2-04	593	172	16.47	12.17	.64
2-06	588	170	15.08	11.14	.60
2-16	587	170	15.88	11.74	.63
Av.	591	169	15.41	11.39	.62

NOTE: 1) Above values of open circuit voltage and short circuit current are not derived from the I-V curve but are read separately.

2) Lot Ø printed with six grid lines per cell with approx. .010" line widths. Lots 1 and 2 printed with eight grid lines per cell and approx. .005" line widths.

Table 14

Data for Boiling Water Test of Screen Printed Wraparound Contact Silicon Solar Cells

Cell No.	Test Condition	V_{oc} (mV)	I_{sc} (mA)	Max.Pwr. Density (mW/cm^2)	Calculated Efficiency	Calculated Curve Factor
1-01	Initial	585	161	14.62	10.8	.62
	Post Boil	---	---	-----	----	---
	Post Etch*	584	161	14.00	10.3	.60
1-02	Initial	592	171	14.70	10.9	.58
	Post Boil	593	171	14.02	10.4	.55
	Post Etch*	591	170	14.52	10.7	.58
1-04	Initial	592	170	12.94	9.6	.51
	Post Boil	---	---	-----	----	---
	Post Etch*	593	170	12.58	9.3	.50
1-05	Initial	591	155	11.87	8.9	.52
	Post Boil	593	155	11.14	8.2	.48
	Post Etch*	591	155	11.55	8.5	.50
1-07	Initial	591	162	14.77	10.9	.62
	Post Boil	---	---	-----	----	---
	Post Etch*	588	161	13.57	10.0	.57
Av.	Initial	590	164	13.78	10.2	.57
	Post Boil	---	---	-----	----	---
	Post Etch*	589	163	13.24	9.8	.55

NOTE: 1) Test consisted of immersing cells in boiling deionized water for ten minutes and drying. Cells were measured before ("initial") and after immersion ("post boil"). Three cells indicated short after boiling. All cells were then edge etched and tested again to yield the "post etch" data marked (*).

2) All cells were tape peel tested with Scotch brand #600 tape after these tests with no failures.

Table 15

Data for Thermal Shock Test of Screen Printed
Wraparound Contact Silicon Solar Cells

Cell No.	Test Condition	V_{oc} (mV)	I_{sc} (mA)	Max.Pwr. Density (mW/cm^2)	Calc. Eff.(%)	Calc. CFF
Ø-03	Initial	594	167	13.04	9.6	.53
	After Thermal Shock	594	166	14.46	10.7	.59
Ø-08	Initial	589	169	13.47	10.0	.54
	After Thermal Shock	591	168	12.99	9.6	.52
Ø-26	Initial	593	169	14.22	10.5	.57
	After Thermal Shock	593	158	12.54	9.3	.54
Ø-30	Initial	593	168	13.59	10.0	.55
	After Thermal Shock	593	168	13.59	10.0	.55
Ø-32	Initial	592	167	13.89	10.3	.56
	After Thermal Shock	(Cell Broken Prior to Retesting)				
1-12	Initial	594	173	14.43	10.7	.56
	After Thermal Shock	594	171	13.52	10.0	.53
1-13	Initial	594	169	14.30	10.6	.57
	After Thermal Shock	594	168	13.69	10.1	.55
2-11	Initial	593	172	13.89	10.3	.54
	After Thermal Shock	593	171	13.06	9.7	.52
2-12	Initial	591	173	12.97	9.6	.51
	After Thermal Shock	592	170	12.56	9.3	.50
2-17	Initial	585	171	13.93	10.3	.56
	After Thermal Shock	585	170	12.70	9.4	.51
Av.	Initial	592	170	13.90	10.3	.55
	After Thermal Shock	592	168	13.23	9.8	.53

NOTE: 1) Test consisted of immersion in liquid nitrogen for 30 seconds and then in boiling deionized water for 30 seconds, a cycle which was repeated fifteen times with a transfer time of 60 seconds from bath to bath.

2) All cells were tape peel tested with Scotch brand #600 tape with no failures.

4.0 FURTHER TECHNOLOGICAL DEVELOPMENT

4.1 FRONT SURFACE METALLIZATION

Due to the skyrocketing costs of silver it is imperative that an alternative front surface metallization material be developed that has similar characteristics. The cost of the front surface metallization was the only objective laid out at the beginning of the program that was not achieved. The silver paste costs upward of thirteen cents for 60 cm^2 rather than the objective of five cents for 60 cm^2 stated at the beginning of the program. Work on non-silver metallizations was looked at during this contract, but no material tested proved satisfactory. The copper and nickel conductive pastes that were purchased from the Transene Company resulted in extremely poor I-V characteristics, and the aluminum-silicon alloy and molybdenum aluminum alloy pastes tested were also poor performers.

Work currently being done by Milo Macha of Sol/Los Inc. in the Low-cost Solar Array Project under contract with Jet Propulsion Laboratory Inc. shows promise for meeting the cost goals that this program has laid out. He is working on a Molybdenum-tin titanium alloy. This work shows promise for the future as a cost effective alternative, because both molybdenum and tin are roughly one twenty-fifth the cost of silver and the titanium used in the alloy is only present in quantities of one part in ten thousand.

4.2 MINIMUM CELL THICKNESS

There was a minimum of effort devoted to finding the minimum cell thickness that can be successfully screen printed. Further work in this area needs to be accomplished in order to better define the problems associated with the difference in expansion coefficients between aluminum and silicon. Once the thermal mismatch problem and the mechanical interaction of the screen printing machine with the wafer are understood, work can be initiated to minimize these effects.

5.0 CONCLUSIONS

An optimized screen printed contact system for both conventional and wraparound cells was established during this contract. All parts of the process sequence were looked at in order to make the most cost effective cell. Thick Film Systems silver paste A256 with Transene n-diffusol was selected as the front surface metallization that had the best over-all characteristics. Frit content not exceeding five percent and a firing temperature not exceeding 700^{o}C were determined as the optimum characteristics for this paste. Thick Film System #1126RCB was selected as the best dielectric isolation. It was found that a double coating was preferable for filling in pinholes and eliminating shunting effects even though both the double and single coats were judged good in the tests. Work on the back surface field preparation sequence showed that the oxide etch before the alloy step showed no noticeable effect on efficiency and therefore could be considered optional.

Work was also completed investigating the cause of the scatter in open circuit voltages found from time to time between lots of cells where the paste back surface field was supposedly processed in identical ways. Cells that were removed slowly showed a markedly poorer performance than the ones that were removed fast. A fast removal has been incorporated into the process sequence. Wafers with a bulk resistivity of 9 to 14 ohms were used for all cells. Wafers that had a resistivity of 7 to 9 ohms were found too sensitive to the mechanical processes that are associated with screen printing. Investigation into the appropriate gridline density has shown that eight to ten lines per centimeter is the optimum number that allows additional shallowing of the junction.

The minimum cell thickness that could be successfully screen printed (with acceptable yields) was about 2½ to 3½ mils. Cells 1½ to 2½ may be printed without breakage, but the firing frequently results in wafer fracture unless the perimeter is reinforced with greater silicon thickness.

Conventional cells, fabricated under this contract, were able to withstand the conventional Scotch tape peel test, storage at 88°C and 90% relative humidity for ten days, a ten minute immersion in boiling water, and thermal shock consisting of fifteen cycles from -196°C to +100°C at a 20°C minute rate without loss of adhesion. Wraparound cells, fabricated under this contract, were able to withstand both the thermal and boiling water tests, but a lack of funds and time prevented any testing at high temperature and high humidity.

Both the conventional and wraparound cells produced on this contract compared favorably with cells produced in the past with the old batch processing methods. The optimized screen printing process developed in this program shows great promise for application to the mechanized production techniques that will be required on the Solar Electric Propulsion System (SEPS) and the Satellite Solar Power System (SSPS). With the implementation of the process sequence developed under this program, cost could be greatly reduced.

6.0 REFERENCES

1. Elms, R.V., Jr., and Young, L.E., Eleventh IECEC, pp 1372, Sept., 1966
2. "Satellite Solar Power Station", Spectrolab Report Q-71098, Nov., 1971
3. Taylor, W. E., "Demonstration of the Feasibility of Automated Silicon Solar Cell Fabrication", Topical Report, NASA Lewis Research Center, Contract NAS3-18566, NAS CR-134981, Oct., 1975
4. Thornhill, J. W., "Automated Fabrication of Back Surface Field Silicon Solar Cells with Screen Printed Wraparound Contacts", Final Report, NASA Lewis Research Center, Contract NAS3-20029, NAS CR-135202, Aug., 1977